Linear and Nonlinear Optical Properties of Photochromic Molecules and Materials

Jacques A. Delaire* and Keitaro Nakatani

Laboratoire de Photophysique et de Photochimie Supramoléculaires et Macromoléculaires (PPSM, UMR 8531 of CNRS), Ecole Normale Supérieure de Cachan, 94235 Cachan Cedex, France

Received September 2, 1999

Contents

I. Introduction 1817
II. Photoinduced Birefringence and Dichroism 1818
A. Basic Mechanism and Experimental Methods 1818
B. Experimental Results for Polymers Containing Azobenzene Derivatives 1820
C. Self-Assembled and Langmuir–Blodgett Monolayers and Multilayers 1822
D. Dynamics of Photoinduced Anisotropy 1823
E. Applications of Photoinduced Birefringence and Dichroism in Photochromic Materials 1825
III. Photoinduced Surface Gratings on Azo Polymers 1826
A. Experimental Results 1826
B. Models 1827
C. Applications 1829
IV. Molecular Second-Order Nonlinear Optical Polarizabilities of Photochromic Molecules 1829
A. Definitions 1829
B. Methods of Determination of Molecular Hyperpolarizabilities: Experiments and Calculations 1830
C. Influence of Photochromism on Molecular Hyperpolarizabilities 1831
V. Poling of Photochromic Materials for Second-Order Nonlinear Optics 1833
A. General Presentation 1833
B. Photoassisted Poling (PAP) 1834
1. Principle 1834
2. Measurement Techniques 1835
3. Examples 1836
4. Applications 1838
C. All-Optical Poling 1838
1. Principle 1838
2. Photochromes for AOP and Applications 1839
VI. Photoswitching of NLO Properties in Organized Systems and Materials 1839
A. Introduction 1839
B. Photoswitching in Polymers 1839
C. Photoswitching in Other Systems 1841
D. Potential Applications 1841
VII. Conclusion and Outlook 1841
VIII. References 1842

I. Introduction

Incorporating photochromic molecules into organic or hybrid organic−inorganic materials leads to photoresponsive systems, the properties of which can be manipulated by light. Photochromism[1,2] is usually defined as the reversible photoinduced transformation between two molecular states whose absorption spectra are significantly different. Besides this color change, which is the most spectacular evidence of photochromism, many molecular and bulk properties also change along with this transformation, and part of them are dealt with in this special issue of *Chemical Reviews*. For example, at a molecular level, switching of metal ion capture[3] and energy or electron transfer[4,5] can occur as a consequence of a photochromic reaction. As concerns bulk properties, photostimulated viscosity changes or even phase separation is observed in polymeric solutions loaded with photochromes;[6,7] more interesting, photostimulated conformational changes of polymer chains in solutions can induce macroscopic changes in the shape and size of polymers and solids.[7]

This review concentrates on optical properties and applications of photochromic molecules and materials, other than the UV−vis absorption change, but connected with it. During the last 10 years, a lot of new optical phenomena emerged and motivated us to write this review, which covers this 10 year period. Among them, are linear absorbance and refractive index changes in solid systems exploiting ordering effects,[8] and leading to photoinduced birefringence and dichroism, mainly studied in azo polymers.[9] More recently, stable relief surface gratings have been drawn in the same kind of azo polymers.[10,11] The large number of potential applications as reversible optical data storage, diffraction, and holography has stimulated a great deal of experimental and theoretical work, which starts to extend to the use of different photochromic systems. We will survey these applications in linear optics. Then, the domain of nonlinear optical (NLO) properties and applications of photochromes will be dealt with. The extraordinary growth and development of nonlinear optical materials during the past 15 years has rendered photonic technologies an essential part of many components used in our daily life, in computer networks and telecommunication systems.[12,13] Among all the inorganic and organic materials which have been developed recently to reach the best figures of merit, photochromic molecules play a prominent role. First, some of them have large molecular hyperpolarizabilities (first and second). Second, the coupling between photochromism

10.1021/cr980078m CCC: $35.00 © 2000 American Chemical Society
Published on Web 03/10/2000

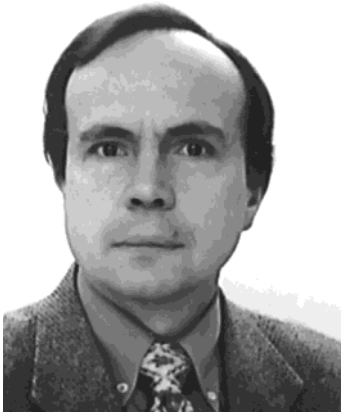

Jacques A. Delaire was born in Chateldon, France, in 1947. He graduated from Ecole Normale Supérieure in Cachan, France, in 1970 and received a Science Doctorate (Doctorat d'Etat) in chemistry from Parix XI University (Orsay) in 1980. He spent 23 years as an assistant professor and a professor at Paris XI University. He was working there first on radiation chemistry in liquids and then on photophysics in polymers, as a member of the Laboratoire de Physico-chimie des Rayonnements (URA 75 of CNRS). In 1983–1984, he spend half a year at the University of Texas at Austin working with Professors S. Webber and M. A. J. Rodgers on photoelectron transfer in polymer solutions. He then cam back to Paris XI University and continued research on photochemical processes in polymers (photoelectron transfer, primary processes in photoresists). After spending one year at the Thomson-CSF research laboratory, he was elected Professor at Paris XI University in 1989. In 1993, he moved to Ecole Normale Supérieure de Cachan, where is is the head of the Laboratory of Photophysics and Photochemistry of Supramolecules and Macromolecules (PPSM; UMR 8531 of CNRS) since 1998. His current areas of interest are photophysics and nonlinear optics of molecular materials, with a special emphasis on the coupling between different properties such as photochromism and nonlinear optics. He is also working on materials for optical limiting and photocatalysis. He is a member of the Editorial Board of the *Journal of Photochemistry and Photobiology, Part A*.

Keitaro Nakatani was born in 1964 in Tokyo, and grew up in Tokyo and Strasbourg, France, where he graduated high school. In 1983, he successfully passed the entrance examination of Ecole Normale Supérieure, Saint-Cloud & Fontenay (near Paris), where he majored in chemistry and obtained Agrégation (French national examination for teaching ability) in chemistry in 1987. His Ph.D. work (1987–1991) was on the synthesis and the magnetic properties of metal complexes under the supervision of the late Professor Olivier Kahn, Laboratoire de Chimie Inorganique at the Université de Paris-Sud, Orsay, In 1991, he joined Professor Jacques A. Delaire's group as a CNRS Chargé de Recherche (Research Scientist), where he started to work on nonlinear optical and photochromic molecules and materials. This research group moved from Orsay to Ecole Normale Supérieure de Cachan (near Paris) in 1993, where he was appointed to a professor position in 1999. He was awarded the Médaille de Bronze from CNRS. Currently, he is involved in research on multiproperty materials (coupling of different properties, for example, photochromism and nonlinear optics) and in projects on new applications of photochromes.

and NLO properties leads to very specific features that can be used in processing materials for second-order NLO:[14,15] for example, creation of noncentrosymmetry, which is a prerequisite for second-order NLO, can be induced by photoassisted poling and all-optical poling. In some cases, photoswitching of NLO properties of photochromic materials can lead to the conception of new devices for data storage or optooptical switching.

II. Photoinduced Birefringence and Dichroism

A. Basic Mechanism and Experimental Methods

The Weigert effect, which is the property of some materials to become dichroic and birefringent when irradiated by polarized light, has been known since the beginning of the century[16,17] in photographic silver emulsions. This photoinduced anisotropy (PIA) was observed in the 1060s in viscous liquids and polymers containing azo derivatives[18,19] and was applied some years later as a potential means of optical data storage.[20,21] Since then, there have been many works dealing with PIA in amorphous and liquid crystalline polymers[9] and mono- and multilayers doped or functionalized with azo derivatives.[22] More recently, a few groups have investigated PIA phenomena in polymers doped with spiropyrans.[23−25] The generally agreed upon mechanism is the following: when irradiated by linearly polarized light, photochromic molecules, considered as anisotropic (or cigar-like-shaped), undergo photoisomerization cycles—for example, trans (or *E*) → cis (or *Z*) → trans—photoisomerization for azo derivatives and change their orientation, tending to line up in a direction perpendicular with the direction of polarization of the excitation (Figure 1). When probed with a polarized light beam, such a medium shows increased absorption and refractive index in a perpendicular polarization direction. Irradiation of the sample with unpolarized or circularly polarized light at normal incidence restores isotropic absorption.

In liquids, this anisotropy would relax quickly, but can persist for a long time in rigid matrixes. PIA can

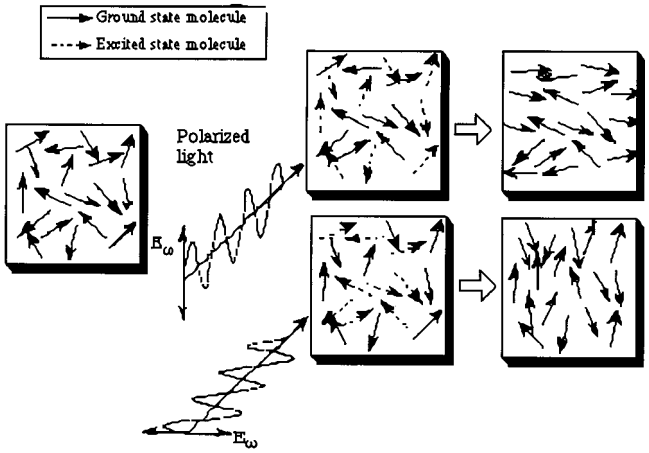

Figure 1. Optical generation of anisotropy. The molecules excited with polarized light tend to align in a direction perpendicular to the polarization.

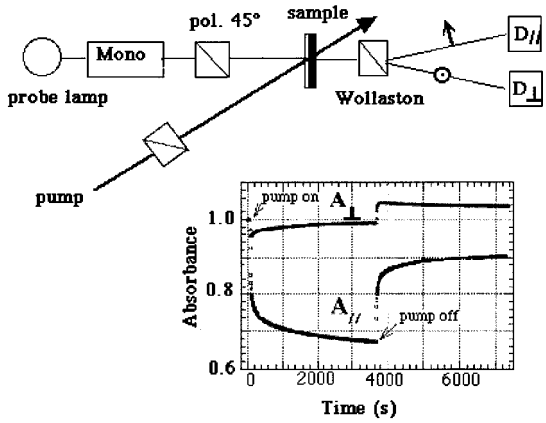

Figure 2. Photoinduced dichroism in polymer films. Upper part: experimental arrangement. Lower part: time evolutions of perpendicular and parallel absorbances during exposure ($I = 10$ mW·cm^{-2}) to a linearly polarized pump beam, for a 5% DR1/PMMA sample (film thickness 1 μm). DR1 stands for Disperse Red One. PMMA stands for poly(methyl methacrylate). Adapted from ref 27.

be quantitatively defined by two quantities: the macroscopic order parameter S

$$S = \frac{A_{\parallel} - A_{\perp}}{A_{\parallel} + 2A_{\perp}}$$

where $A_{\parallel}$ and $A_{\perp}$ represent the absorbance with a polarization parallel and perpendicular to the polarization of the excitation, respectively, and the birefringence

$$\Delta n = n_{\parallel} - n_{\perp}$$

$n_{\parallel}$ and $n_{\perp}$ being the refractive indices for polarizations parallel and perpendicular to the polarization of the excitation, respectively.

Different optical methods have been used to study photoinduced dichroism and birefringence in thin films and monolayers. For dichroism measurements, polymer films, deposited on a glass slide, are pumped by a linearly polarized beam (Figure 2). A probe light beam coming from a white light source and almost parallel with the pumping beam is focused on the sample, and the absorbance is measured for parallel and perpendicular polarizations.[26,27]

In a more sophisticated arrangement,[28] mutiwavelength dichroism analysis could be made without using a too high level of probe light which could destroy the PIA induced by the pumping beam. Different setups have been used for birefringence measurements. In the simplest arrangement,[20,29,30] the sample is placed between two crossed polarizers in the path of a laser (reading) beam chosen at a wavelength out of the absorption spectrum of the photochrome. Another (writing) beam, almost collinear with the preceding one, pumps the photochrome in its absorption band. Photoinduced birefringence creates a change in transmission of the probe beam, this change being maximum when the polarization vector of the pump beam is set to 45° with respect to the polarization vector of the probe beam. Another arrangement consists of creating a grating by irradiation through a photomask made of

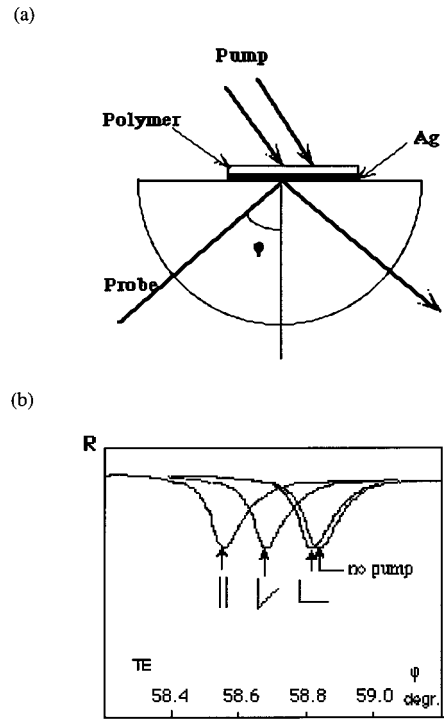

Figure 3. ATR experiment. (a) Experimental setup for pump−probe experiments. (b) Transverse electric reflectivity recorded versus incidence angle: angular shifts of one of the 1.06 μm reflectivity dips, induced by a pump beam at 546 nm with different polarizations compared with the probe beam (parallel, perpendicular, and with an angle of 45°) Adapted from ref 34.

regularly spaced alternating black and white stripes[31] or with an interference pattern,[21,32,33] and then measuring the diffraction of a reading beam by this photoinduced grating. From the measured diffraction angle, a refractive index change can be deduced. A more powerful method uses attenuated total reflection (ATR).[34] This method is a generalization of the Kretschmann method using surface plasmons which are transverse magnetic waves propagating along a metal−dielectric interface, their field amplitudes decaying exponentially perpendicular to the interface. These free waves can be coupled with guided waves in the thin organic layer (amorphous polymer or Langmuir−Blodgett−Kuhn layer). Resonance conditions allow very accurate determination of the refractive index (accuracy $<10^{-3}$) and thickness, and are very sensitive to any changes occurring inside or at the surface of the film. Figure 3 shows the experimental setup.

The sample is a glass slide coated with a gold layer on which the organic layer is deposited. For further determination of electrooptical coefficients (see section V), a second gold layer is deposited on the top of the organic film. The glass face of the slide is put in optical contact with a half-sphere. The reflectivity of a He−Ne or near-infrared diode laser beam is measured through the half-sphere, as a function of the incidence angle. The angular positions of the dips in reflectivity (Fabry−Perot dips), with polarization perpendicular (transverse electric, or TE) or parallel (transverse magnetic, or TM) to the incidence plane, give the three components of the refractive index and the thickness of the films.[22,34,35] Photoinduced bire-

fringence induces a shift in the angular position of the dips, from which changes in the refractive indexes (and thicknesses) can be determined.

B. Experimental Results for Polymers Containing Azobenzene Derivatives

The kinetics of photochemical and thermal isomerization of azo compounds has been well investigated experimentally, and the results have been compared for azo dyes dissolved in solutions or dispersed in polymers with the same azo dyes covalently bound within the polymer backbone or attached to the backbone.[9,36,37] According to Rau,[38] there are three different classes of azobenzene derivatives, depending on the relative energetic order of their (n,π*) and (π,π*) states: azobenzene-type, aminoazobenzene-type, pseudo-stilbene-type. The first class (azobenzene-type) is characterized spectroscopically by a low-intensity n$-\pi$* band in the visible region, well separated from a high-intensity $\pi-\pi$* band in the UV. In these molecules, the back thermal $Z \rightarrow E$ reaction is very slow, specially in polymers. In the second class (aminoazobenzene-type), both n$-\pi$* and $\pi-\pi$* bands overlap, while for the third class (pseudo-stilbene-type), the order of energies of both transitions is reversed. In aminoazobenzene- and pseudo-stilbene-type molecules with the push/pull substituents (see section IV), the *Z* state isomerizes back very quickly (from several milliseconds in solution to a few seconds in polymer matrixes). The metastability of the *Z* state plays a dominant role in the interpretation of photoinduced phenomena in azo polymers, and also in the kind of optical information storage which can be envisaged using these polymers. Indeed, for induction and modulation of the molecular alignment of liquid crystals by light, azo compounds with stable *Z* isomers are used.[39] On the other hand, for optically induced birefringence and dichroism, we will see that azo compounds whose *Z* state reverts back quickly to the *E* state are preferred.

Two alternate mechanisms have been suggested for photoisomerization. The first one is similar to the one proposed for alkenes and implies that the azo aromatic group isomerizes by rotation about the $-$N$=$N$-$ bond. The second mechanism implies inversion of one or both of the nitrogens. This second mechanism is often thought to be responsible for the high quantum yields ($\Phi_{E\rightarrow Z}$ and $\Phi_{Z\rightarrow E}$) of $E \rightarrow Z$ and $Z \rightarrow E$ isomerization reactions in polymers, respectively, far below the glass transition temperature (T_g) of these polymers. It is indeed surprising to find almost similar values in solutions and in polymer matrixes for the quantum yields $\Phi_{E\rightarrow Z}$ ($\approx$0.1) and $\Phi_{Z\rightarrow E}$ ($\approx$0.5).[40,41]

The first photochromic polymer used as an optical recording medium contained an azo dye (methyl red or methyl orange) dispersed in a matrix of poly(vinyl alcohol).[20] In this system, optical dichroism and birefringence have been observed; however, the PIA only lasts a few tens of seconds. Using a liquid crystalline (LC) polymer whose structure is depicted in Figure 4, Wendorff et al.[32] were able to perform optical storage experiments by irradiation with linearly polarized light at room temperature. The

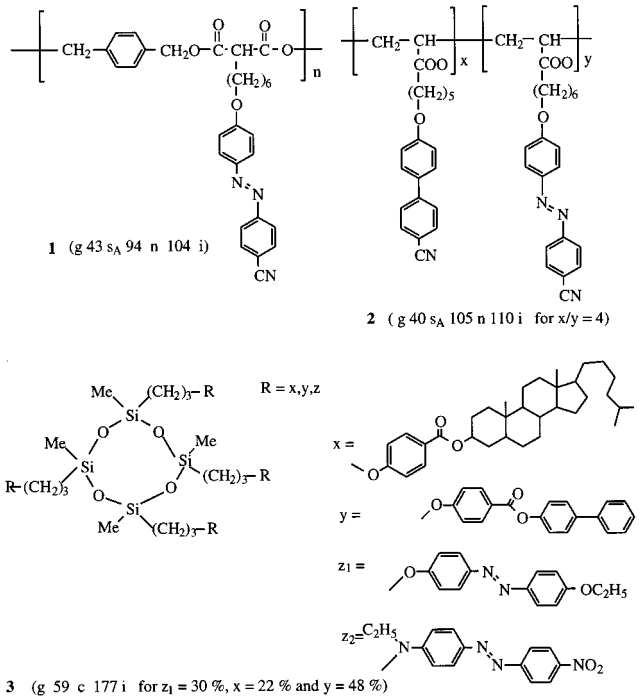

Figure 4. Liquid crystalline azo polymers studied for their PIA properties: **1**, polyester;[32] **2**, copolymers of acrylates;[45] **3**, cyclic cholesteric tetramethylsiloxanes;[51] g, glassy; n, nematic; s_A, smectic A; c, cholesteric; i, isotropic.

polymer was previously oriented under an appropriate electric field above T_g. In such conditions, the stored pictures were stable until the sample was heated above the nematic$-$isotropic transition temperature. Since this work, there have been a lot of developments in the same area, and different structures of LC nematic polyesters and polyacrylates,[42−50] or cholesteric polysiloxanes,[51] have been synthesized (see Figure 4 for some of these structures).

In all these systems, PIA was induced by irradiating the preoriented LC polymer with linearly polarized light at a temperature above T_g. The isomerization of the azo groups is thought to affect the LC orientation. In addition, it was shown that the optical axis of the LC polymer changes to be perpendicular to the polarization direction of the irradiating laser light. In other systems, LC copolymers were synthesized with azo side groups and nonphotosensitive side groups, and it was shown that the reorientation of the azo groups actually influences the neighboring mesogenic groups either above T_g[52] or above and below T_g.[45,46] This cooperative effect on the neighboring group is due to the long-range elastic forces existing between the mesogenic groups and the azo groups.[53] Control of LC alignment by optical means is a very exciting challenge; the above-mentioned works have shown that it can be done with azo dyes dispersed in the bulk of a LC polymer, and the competition of self-organization and photoorientation in LC polymers has been studied in detail during the past five years.[54−56] Control of LC alignment can also be done in the alignment surface, and this very important topic will be developed in the review by Dr. Ichimura in this issue.

The notion of "molecular addressing" was introduced at that time by Anderle et al.,[52] which means

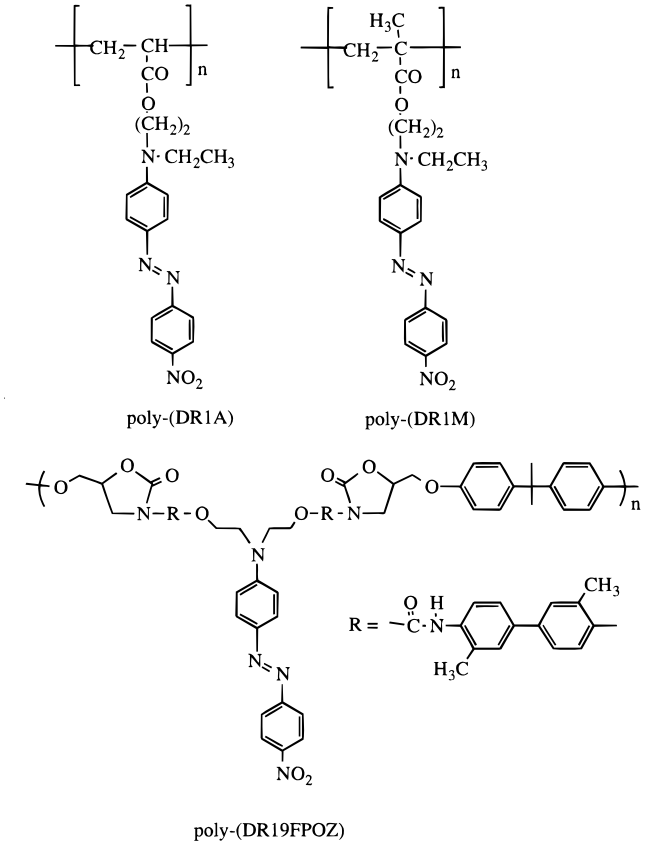

Figure 5. Structure of some azo polymers with T_g higher than room temperature. The first two, poly(DR1A) and poly(DR1M), have been used in many studies as homopolymers or copolymers with poly(methyl acrylate) (PMA) or PMMA.[58−78] Poly(DR19FPOZ) has been used in ref 30.

that, according to these authors and in contrast with the conclusions of others,[45,46] only azo groups were "addressed " below T_g. This controversy has been explained recently by the study of cooperative motion in amorphous polymers[57] as we explain below. Indeed, PIA has been studied at room temperature in different amorphous azo polymers[40,58−78] which have high T_g temperatures. The structure of some of these polymers is given above (Figure 5).

It has been shown that, first, polymers doped with azo derivatives, such as DR1, did not give stable PIA (only 35% of the orientation is conserved 1 h after the end of irradiation); on the contrary, the same polymer with covalently linked azo groups gives stable PIA (80% of the orientation is conserved).[70,71] Second, the higher the T_g, the larger the stability of the written material, so it has been demonstrated that PIA does not require liquid crystalline polymers. The written information can be erased either by heating the material above T_g or by irradiating it with circularly polarized light. Going back to the molecular addressing controversy, Natansohn et al. have studied PIA in two kinds of copolymers (Figure 6): polar azo/polar ester copolymers (such as poly(DR1M-*co*-BEM)) in comparison with polar azo/nonpolar ester copolymers (such as poly(DR1M-*co*-NBEM)).[57]

These results have demonstrated the existence of a cooperative motion to a great degree in the poly(DR1M-*co*-BEM) system and to a much lesser degree

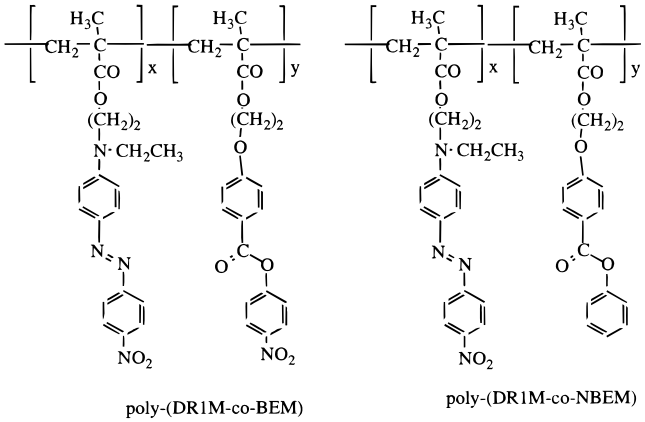

Figure 6. Structure of two copolymers used for the study of molecular addressing in PIA.[57]

in poly(DR1M-*co*-NBEM), indicating the major role played by the driving force of dipole−dipole interactions. Consequently they explained the molecular addressing observed by Anderle et al.[52] by the nonpolarity of the azo group that they used; on the other hand, Wiesner et al.[45] used a polar azobenzene and a polar ester (Figure 6).

The influences of different structural and external parameters have been examined in azo polymers, to achieve the highest and most stable birefringence and/or dichroism. For example, Natansohn et al.[63] studied the effect of the size of the photochromic groups: they compared two polymers: poly(DR1M) and a similar polymer with a nitronaphthyl group instead of the nitrophenyl group (poly(NDR1M)), and

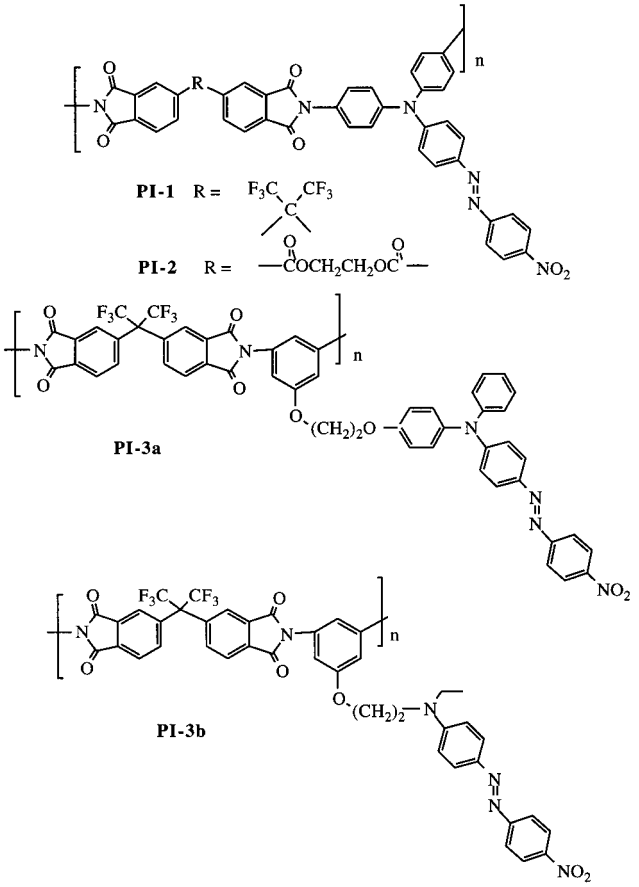

Figure 7. Structure of azo polyimides studied in PIA.[79−81]

they found that the bulkier poly(NDR1M) exhibited a slower writing rate, but there was no significant difference in the maximum birefringence achieved and in the relaxation rate. The same authors[68] synthesized a copolymer of methyl methacrylate containing a rigid group with two azo bonds, and measured a photoinduced birefringence higher by a factor of 5 than the birefringence inducible in a typical azo homopolymer containing a chromophore with only one azo group.

As the relaxation of the orientation is related to the free volume in the polymer, it is interesting to increase the T_g to freeze almost all molecular movement of polymer segments at room temperature. The problem is that photoisomerization can also be hindered and become so slow that any PIA is prevented. It has been found that photoisomerization of azobenzene derivatives still occurs in high-T_g polyimides, whose structure is given in Figure 7.[79−81]

These polyimides differ in the method of incorporation of the azo chromophore into the polyimide (PI) backbone. In PI-1 and PI-2 (T_g = 350 and 252 °C, respectively), the chromophore (an azo group with donor and acceptor substituents) is incorporated rigidly into the backbone without any flexible connector, or tether. PI-3a and PI-3b (T_g = 228 and 210 °C, respectively) on the other hand are side-chain polyimides where the azo dye is tethered to the main chain via a flexible tether. The authors have shown that, in all these copolymers, $E \rightarrow Z$ photoisomerization occurs, even 325 °C below T_g in PI-1. PIA is also observed in the four systems after irradiation with the polarized green light of a frequency-doubled Nd^{3+}: YAG laser, but in contrast to PI-3b films, which do show some relaxation of the nonpolar orientation, a quasi-permanent orientation was induced in PI-1 and PI-2. We will see further the advantage of these high-T_g polyimides for second-order nonlinear optics (see section V). Natansohn et al.[82] also compared PIA in films containing DR1 doped into poly(methyl methacrylate) and into a high-T_g poly(ether ketone) (pASH; T_g = 265 °C) and observed a high stability for the PIA in a pASH matrix. They also synthesized a polyester (pMNAP) of bisphenol A and of 3-[4-(4-nitrophenylazo)phenyl]-3-aza-pentanedioic acid (T_g = 152 °C) in which a fairly low birefringence relaxation occurs. Unfortunately, this polyester decomposes at about 160 °C, which prevents its use as a material for optical storage.[67]

The effects of temperature,[30,83] irradiance,[27,30,55,83,84] and film thicknesses[30,85] on PIA dynamics and efficiency have also been studied recently. It has been shown that the growth and decay of birefringence signals can be fitted by a biexponential.[58] Song et al.[30] found no change in rate constants for different pump irradiations; their data also show that the amplitude of the exponential describing the fast process increases linearly with pump irradiance. On the contrary, Natansohn et al.[58] found that both rate constants of the biexponential growth increase with increasing irradiance, as predicted by a simple three-state model (see below). These authors also pointed out that the three irradiance values used by Song et al. were in a domain which may appear linear in their results as well. Lagugné Labarthet et al.[27] have shown that the rate constants for birefringence are not connected with the rate constants of the $E-Z$ photochemical reaction, which can also be described by a biexponential kinetics; they concluded that the values of the rate constants for birefringence growth were modulated by the rotational diffusion constants. As concerns temperature influence, Natansohn et al.[83,84] found that the absolute value of the photostationary order parameter decreases monotonically as a function of temperature, approaching zero as the systems restore their isotropic distribution of chromophores around T_g. The rate constant for the fast process increases with increasing temperature for one of the polymers studied (poly(MEA)), and decreases for another one (poly(DR1M)). These opposite variations were interpreted as the result of two competing processes: on one hand, there is alignment due to the polarization of the laser; on the other hand, there is a tendency toward disorder and restoration of the equilibrium isotropy. Dipolar interactions present in poly(DR1M) seem to be the origin of the decrease of the rate constant for increasing temperatures. The same authors found no clear variation of the rate constant of the slow growth with temperature. On the contrary, Song et al.[30] found that both fast and slow rate constants had positive and almost equal activation energies (29 ± 2 kJ·mol^{-1}). Film thickness also influences the maximum birefringence obtainable and growth rates. Natansohn et al.[83,84] argued that, due to large laser intensity absorption by the azobenzene moiety, the intensity of the writing beam decreases rapidly as it propagates through the specimen, thus leading to a decrease in rate constants. However, Song et al. did not find any variation of rate constants with film thickness. They only found a variation of preexponential factors.[30]

Recently, Ishitobi et al.[86] have shown that it is possible to individually address the photoinduced orientation of two different photochromes (diarylethene and spiropyran) in the same polymer (PMMA) by irradiating with UV and visible light, thus opening a new field of investigation in photochromic systems.

C. Self-Assembled and Langmuir–Blodgett Monolayers and Multilayers

Since the first studies of Blair et al.[87] dealing with the photoresponse of mixed monolayers of some polymers with photochromic spiropyrans and azo polymers, a lot of work on monolayers containing different photochromes has been done, stimulated by the research on command surfaces for liquid crystal alignment.[88] As this topic will be developed in another review (see the review by Ichimura in this issue), we will focus here on the studies dealing with photoinduced dichroism and birefringence in monolayers and multilayers.

Self-assembled monolayers (SAMs) are molecular films prepared by immersing a suitable substrate into a solution containing surface active molecules (azosilane). The molecules then self-assemble at the solid−solution interface to a well-organized monomolecular layer with a structural order comparable

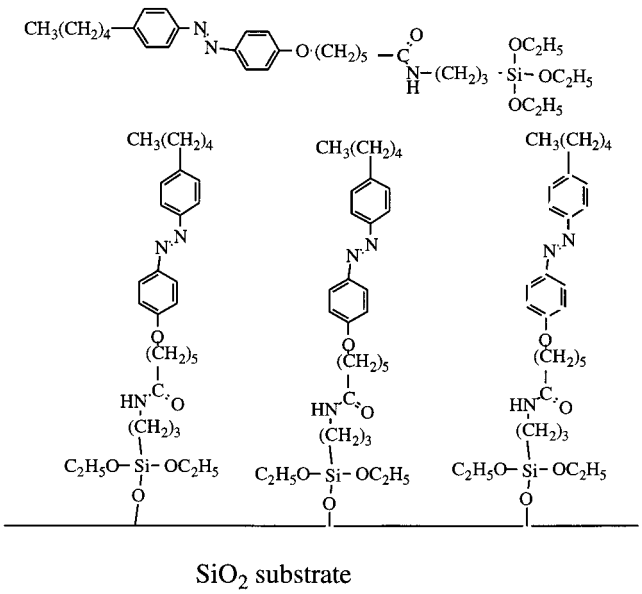

Figure 8. Top: structural formula of 4-[6-carboxy-(3-amidopropyl)triethoxysilane]-4′-pentylazobenzene, referred to in the text as azo-silane, which leads to a self-assembled monolayer. Bottom: idealized schematic drawing of a SAM on a SiO_2 substrate.[89−91]

to that of Langmuir films. Many examples are based on the O−Si bond formation between the silyl headgroup of amphiphile molecules and the polar silanol groups on glass or quartz substrates.[89−91] One example of such a structure is given in Figure 8, with the hydrophobic tail bearing the azobenzene derivative.

In these monolayers, the photoisomerization of the azobenzene group still occurs with a *Z* state thermally stable over several hours. UV dichroism and optical anisotropy are observed. Furthermore, it was possible to follow the change of optical thickness during irradiation of the sample with UV light, which gives information about the reaction rates.

Amphiphilic molecules can be deposited as monolayers at the air−water interface. These layers can be transferred to a solid support by dipping and withdrawing a suitable substrate through this well-organized film. These so-called Langmuir−Blodgett−Kuhn (LBK) layers have been studied during the last 20 years for potential applications in optical storage,[92] nonlinear optical properties,[93] and command surface of liquid crystal cells (see the review by Ichimura in this issue). Various techniques have been developed for the optical characterization of such ultrathin coatings.[94−96] As an example, photochromic azo-polyglutamate polymers are "hairy-rod" structures (Figure 9) with azo groups in the flexible side chains.[97,98] In LBK layers, the rods are oriented parallel to the dipping direction and the side chains form a liquidlike matrix.[99,100] Reversible photoinduced birefringence was observed in these multilayers by the ATR technique: initial anisotropy induced by the depositing technique (out-of-plane refractive index being larger than the in-plane ones) was turned off by UV irradiation, and was restored under blue irradiation.

However, in these LBK layers, no photoselection was observed, contrarily to the same systems deposited as amorphous films by the spin-cast technique.[78] In other words, the changes of anisotropy observed in the LBK films were insensitive to the polarization of the exciting light; this was interpreted as a consequence of the subtle manner of reorientation of the azo units imposed by the LBK deposition technique.

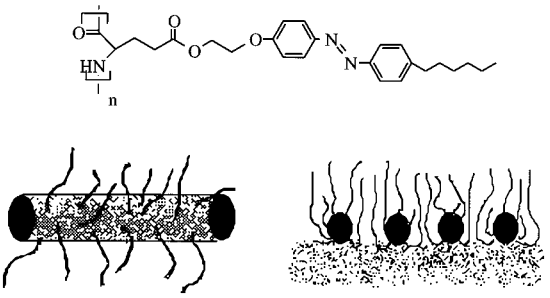

Figure 9. Chemical structure of the azo-polyglutamate (top), schematic view of the hairy-rod-type polymer structure (bottom left), and structure of the LB layer on the water surface (bottom right).[99,100]

D. Dynamics of Photoinduced Anisotropy

On the basis of mechanisms found for azo dyes in polymers, M. Dumont et al.[70−72] developed a theoretical mean field model to describe the phenomenon of PIA. It is based on a simple four (electronic) level diagram, which takes into account *E* (trans) and *Z* (cis) populations of photochromes, and their excited states, which are supposed to have a negligible lifetime (Figure 10). This model could also be applied to other photochromic systems, like spiropyran/photomerocyanine.[101]

Three different processes have been considered in this model: angular hole burning (AHB), angular redistribution (AR), and rotational diffusion (RD). Angular hole burning is due to the strongly anisotropic polarizability of the trans azo dye, whose transition dipole moment is oriented along the long axis of the molecule.[41] A linearly polarized light beam selectively pumps molecules whose transition dipole moment axis is parallel to its polarization (probability $\propto \cos^2 \theta$). As part of the excited trans molecules may relax to the ground state of the cis isomer, which has a relatively long lifetime (from a few seconds to infinity, depending on the photochrome), optical pumping produces an anisotropic depletion of the angular distribution of the trans isomer: this is AHB. As cis molecules generally absorb at the same wavelength, they can also be excited, but for the cis isomer of cyanomethoxyazobenzene, it has been shown that the polarizability tensor is almost isotropic,[41] which will imply no AHB for the cis form. If AHB is the only mechanism, anisotropy disappears with the lifetime of the cis state. Experimentally, anisotropy has a longer lifetime than the cis state[27] in doped polymers and can be permanent in copolymers. This can be explained by a rotation of the molecules during the trans → cis → trans photoisomerization cycle. This rotation (AR) may be spontaneous during the lifetime of the cis state, which is more spherical, but a more realistic explanation is now that reorientation occurs during the isomerization reactions. In the

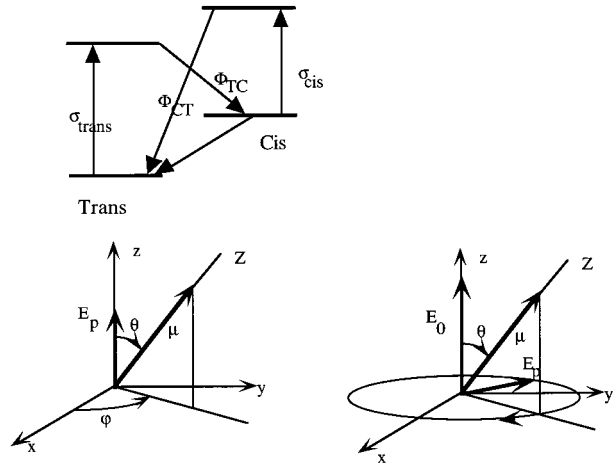

Figure 10. Top: four-level model for the photoisomerization process of azobenzene. Φ_{TC} and Φ_{CT} are the quantum yields for trans−cis and cis−trans conversions, respectively, and σ_{trans} and σ_{cis} are the absorption cross sections for trans and cis states. Bottom: geometry for PIA (left, excitation electric field E_p parallel to the z-axis; right, E_p in the xy plane, with a circular polarization). μ is the ground-state dipole moment of the molecule, and E_0 is the static electric field parallel to the z-axis in the case of photoassisted poling (PAP; see section V).

absence of external field (which will not be the case in photoassisted poling; see below), the rotation is isotropic with respect to the initial direction of the trans molecule, but after several trans → cis → trans cycles, the result is an accumulation of molecules in the direction of the smallest probability of pumping, i.e., the direction perpendicular to the pump polarization direction, so AR amplifies and perpetuates the anisotropy created by AHB. On the reverse, rotational diffusion (RD), which is the rotational Brownian motion of molecules resulting from thermal agitation, tends to randomize the orientation and then to fill the distribution holes.

Two differential equations couple the angular distributions $n_T(\Omega)$ and $n_C(\Omega)$, for the trans and cis species, respectively ($\Omega = \{\varphi,\theta,\chi\}$). These equations include AHB with $\Pr(\Omega)$, which is the probability of pumping a molecule which is oriented with Euler angle Ω, AR with the terms R_{TC} and R_{CT}, and RD with the Smoluchowski diffusion operator (last term of both equations):

$$\frac{dn_T(\Omega)}{dt} = -\Phi_{TC}\Pr(\Omega) + \frac{1}{\tau_C}\int R_{CT}(\Omega'\to\Omega)\, n_C(\Omega')\, d\Omega' + D_T\Delta n_T \quad (1)$$

$$\frac{dn_C(\Omega)}{dt} = \Phi_{TC}\int R_{CT}(\Omega'\to\Omega)\, \Pr(\Omega')\, n_T(\Omega')\, d\Omega' - \frac{1}{\tau_C}n_C(\Omega) + D_C\Delta n_C \quad (2)$$

Φ_{TC} is the quantum yield for trans to cis photoisomerization, τ_C is the lifetime of the cis state, and D_T and D_C are the rotational diffusion coefficients of the trans and cis states, respectively. In this simple model, excitation of cis molecules at the pumping wavelength is not taken into account, but it could be done by adding an AHB term in the second equation (probability of excitation of cis molecules) and an AR term in the first equation (AR of cis molecules arriving on trans molecules).

To simplify the problem, it has been supposed that PIA presents an axial symmetry, which is the direction of polarization of the light in the case of linearly polarized light, or a direction perpendicular to the plane of polarization in the case of circularly polarized light (or unpolarized light, which is the same as far as one does not deal with chiral molecules) (Figure 10). Therefore, the angular distribution of molecules only depends on the θ angle (as far as molecules have an axis of symmetry). It is then possible to use the formalism of order parameters by projecting $n_T(\theta)$ and $n_C(\theta)$ on Legendre polynomials P_q:

$$n_T(\theta) = \frac{1}{4\pi}\sum(2q+1)T_qP_q(\cos\theta)n_C(\theta) = \frac{1}{4\pi}\sum(2q+1)C_qP_q(\cos\theta) \quad (3)$$

In this equation, T_q and C_q are the usual normalized order parameters multiplied by the density of the trans and cis states, respectively. For example, $T_0(C_0)$ represents the population of the trans (cis) state, and T_2 represents trans anisotropy ($T_2 = (A_{\parallel}^{trans} - A_{\perp}^{trans})/3$). The main interest of this method is that the optical susceptibilities of order n ($\chi^{(n)}$) can be expressed easily as a function of these order parameters (parameters of parity $n+1$, up to $n+1$ for $\chi^{(n)}$).[26,102] The probability of excitation $\Pr(\theta)$ can be expressed as a function of $\cos\theta$ in the case of a linearly polarized pumping beam:

$$\Pr(\theta) = I_p(\sigma_\perp + (\sigma_\parallel - \sigma_\perp)\cos^2\theta) \quad (4)$$

I_p is the pump intensity, and σ is the absorption cross section, with two different components, $\sigma_\parallel$ and $\sigma_\perp$, in the case of an anisotropic molecule.

The projection of eqs 1 and 2 on Legendre polynomials leads to a set of coupled equations:

$$\frac{dT_q}{dt} = -\sum_{q'}\Pr_{qq'}T_{q'} + \frac{1}{\tau_c}\sum_{q'}R_{qq'}^{CT}C_{q'} - q(q+1)D_TT_q \quad (5)$$

$$\frac{dC_q}{dt} = -\sum_{q'q''}R_{qq'}^{TC}\Pr_{q'q''}T_{q''} - \frac{1}{\tau_c}C_q - q(q+1)D_CC_q \quad (6)$$

$\Pr_{qq'}$ are matrix elements calculated from eq 4. $R_{qq'}^{XX}$ are rotation matrixes whose expression depends on the model taken for AR. Indeed, this model must represent isotropic spreading of the angular distribution of excited molecules. Dumont et al. considered a fictitious intermediate state which is diffusing with its own diffusion coefficient.[74]

Resolution of eq 5 and 6 has been made after reduction to a finite set of coupled equations by neglecting T_q and C_q for q larger than q_m. This last value is chosen large enough to keep a good accuracy of the calculated susceptibilities (for example, $q_m = 4$ for the calculation of the third-order susceptibility

$\chi^{(3)}$). The solution of the system which then contains $2q_m + 1$ equations is a sum of $2q_m + 1$ exponentials which are computed numerically. This model has been used by different authors for numerical simulations of the dynamics of the increase and relaxation of both photoinduced dichroism and birefringence.[35,103,104] In a very simplified model where the above system of differential equations is truncated above $q_m = 2$ and where angular redistribution is neglected, Sekkat and Dumont[72] obtained an analytical solution which gives biexponentials with the same rate constants for the time evolution of the trans population, $T_0(t)$, and for the dichroism, $T_2(t)$, in the case where one considers almost spherical cis molecules ($C_2(t) = 0$).

Several questions have been raised concerning these models. First, the two state model has been shown to be inefficient to explain birefringence induced in side-chain liquid crystalline polymers.[105−107] For example, Fei et al.[107] investigated the azo dyes methyl orange and ethyl orange in a poly(vinyl alcohol) matrix. They induced a weak holographic grating by excitation of the sample with an argon ion laser at 514 nm and made a subsequent irradiation with two intersecting He−Ne beams at 633 nm. From the observed increase of the diffraction efficiency after the second irradiation, the authors speculate that a two-photon process involving a triplet−triplet transition from a metastable triplet state was at the origin of this biphotonic holographic recording. However, a detailed investigation of the energy levels and lifetimes of the excited states of methyl red[108] gives no indication for the population of higher triplet states. Moreover, holographic recording was repeated with the same arrangement with 4-amino-4′-nitroazobenzene in polycarbonate, and the increase of diffraction efficiency was attributed to the excitation of cis isomers.[109] Second, the preceding model is a uniaxial model which supposes that the orientation distribution induced by linearly polarized light is isotropic around this direction. However, photoinduced biaxiality has been observed on liquid crystalline copolymers containing cyanoazobenzene and cyanophenyl benzoate side chains,[110] in which the mesogens are preferentially aligned perpendicular to the film plane. This biaxiality is the result of the cooperative motion of photochemically active and inert groups discussed above,[60] so there is a need for a deeper investigation of the molecular orientation of photochromes in polymers. Raman scattering has proved to be efficient to obtain higher order parameters (T_2 and T_4) than those obtained by dichroism and birefringence (T_2).[111] Polarized infrared spectroscopy has been recently applied to irradiated azo polymers.[45,112−117] This technique allows the orientation of the IR active groups of both azo chromophores (NO_2, C−N of C−NH_2) and polymer groups (carbonyl and phenylene groups) to be determined in real time. For example, in the copolymer poly(DR19T) (Figure 11), time-resolved FTIR has shown that the different groups of the azo chromophore are oriented perpendicular to the direction of the laser polarization, as expected, and a cooperative orientation of the phenylene diacrylate groups with the azobenzene side chains is observed; it has also confirmed a biaxial orientation distribution of azobenzene groups.[113,114] In PMMA doped with DR1, the results obtained by IR spectroscopy reveal that different chemical groups of the azobenzene molecules display a similar dynamics during both the orientation and the relaxation periods, indicating that the DR1 molecules move as a whole.[115] The study of poly(DR1A-*co*-MMA) copolymers (see Figure 11) shows that isolated azo groups orient more readily than those in interaction with neighboring chromophores.[115]

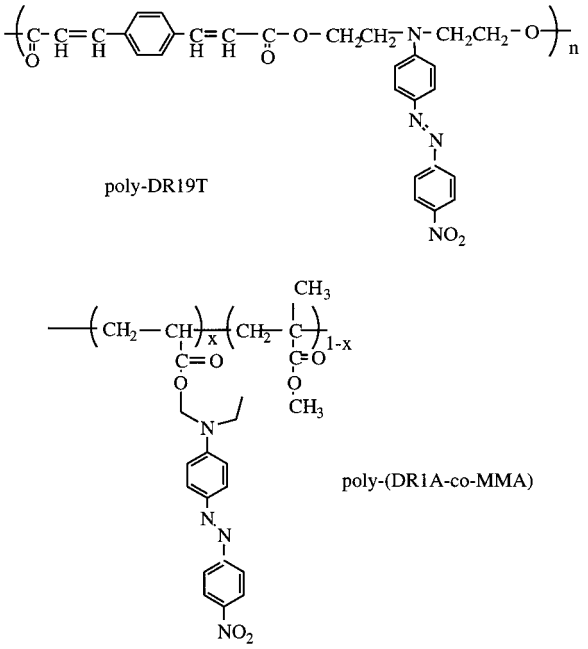

Figure 11. Structures of poly(DR19T) and poly(DR1A-*co*-MMA).

E. Applications of Photoinduced Birefringence and Dichroism in Photochromic Materials

The first application was developed by Todorov et al.,[20,21] who used azo polymers to register polarization holograms. Such holograms are recorded with two interfering light beams whose linear or circular polarizations are perpendicular, contrary to "ordinary" holographic gratings where both beams have parallel polarizations. In the last case, the light intensity is sinusoidally modulated; in contrast, in the first case, the intensity of the resulting light field is constant, and only its polarization is periodically spatially modulated in accordance with the change of phase shift between the two beams. In azo polymers, this modulation creates a spatially modulated refractive index anisotropy. Polarization holography was thought to give higher efficiencies (up to 35%) than ordinary holography, because of the strong absorption of photochromes, which limits the penetration of light in the depth of the films. However, ordinary holography has also been developed in liquid crystal polymers,[32] and because of cooperative effects described above, efficiencies as high as 80% have been obtained.[118]

Photoinduced birefringence in copolymers with azo derivatives has also been proposed for reversible optical data storage[29,51,119−122] as PIA can be created

and erased many times, as long as photodegradation processes are avoided.

Photoinduced birefringence can also be used to pattern optical waveguides,[123−125] which are necessary for the development of passive and active devices in integrated optics for telecommunications. Besides photoinduced birefringence, photobleaching[126,127] or a photoinduced homogeneous refractive index change of materials doped with different photochromes[128−130] has also led to the fabrication of efficient waveguides and optical elements. The relative contribution of the isotropic and anisotropic parts of photoinduced changes in the refractive index of azo dye/polymer systems has been determined,[128] and it has been concluded that the induced anisotropy is related to the dye molecules which are involved in reversible photoisomerization, whereas the isotropic changes, which are stronger, are related to the polymer matrix as well.

III. Photoinduced Surface Gratings on Azo Polymers

A. Experimental Results

In the previous paragraph, we have shown that it is possible to produce volume holographic gratings due to the change in refractive index and/or photoinduced birefringence. Liquid crystalline or amorphous azo polymers doped or functionalized with chromophores are particularly efficient materials. In 1994, Rochon et al.[131,132] found that large surface relief gratings could be directly recorded at room temperature on azobenzene-containing polymer films using two interfering polarized Ar ion laser beams. Tripathy et al.[133−135] have also produced high-efficiency surface gratings from azo side-chain high-T_g polymers. The experimental setup used by these authors and an example of a surface relief grating registered by this method and observed by atomic force microscopy (AFM) are given in Figure 12.

The gratings were optically inscribed onto the films with a single beam of an argon ion laser (488 nm, irradiation power varied between 1 and 100 mW) split by a mirror and reflected coincident onto the film surface which is fixed perpendicular to the mirror. Quarter wave plates are used to change the beam polarization from linear to circular, and the diffraction efficiency is monitored by measuring the first-order diffracted beam of a 1 mW, 633 nm beam from a He−Ne laser. Changing the incidence angle of the writing beam allows the intensity profile spacing on the sample, and then the grating spacing, to be changed. In such conditions, irradiation of the polymer films during a few seconds with intensities of 5−200 mW·cm^{-2} produces reversible volume birefringence gratings (see section II), with low diffraction efficiency (less than 1%). If the film is exposed to the writing beam for longer than a few seconds, an irreversible process begins, creating an overlapping and highly efficient surface grating written on the time scale of minutes, so there is an initial and rapid growth (on the order of seconds) corresponding to the production of the reversible volume birefringence grating, and then a slower and irreversible process (of the order of minutes) which creates surface gratings observable by AFM, with efficiencies up to 50%. It has been established that the phase relationship between the surface and volume gratings is such that the light intensity maxima of the fringes coincide with the surface profile minima.[132] Also, from dynamical experimental studies and polarization analyses of the transmitted ±1 order diffraction beams during recordings, the contributions of the two distinct processes (i.e., the formation of a birefringence grating and of a surface relief grating) have been clearly characterized, and quite interesting different results on DR1 dye-doped and -functionalized polymer films have been put into evidence.[136] Once written till saturation of the diffraction efficiency, the grating profile is not photoerasable either by linearly or circularly polarized light or by long-term exposure to moderate power probe beams. However, if the gratings are inscribed at modest intensities, Tripathy et al.[137] demonstrated that it was possible to erase the gratings under specific polarization conditions for both the writing beam and the erasing beam. In any case, the gratings can be erased thermally by heating the polymer film to T_g. Once a grating is written, another grating can be inscribed, superposed on the first one. Up to 10 coincident gratings have been stored with good resolution.[138] Tripathy et al.[134] and Barrett et al.[138] agree that, when exposed to the same fluence and intensity of light, the samples with grating spacing near 0.8 μm present the largest surface modulation depth.

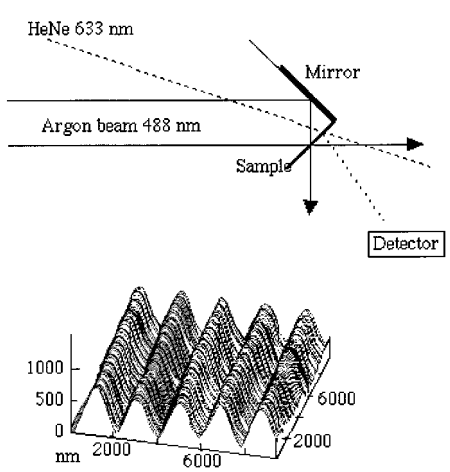

Figure 12. Optically inscribed diffraction gratings in azo polymer films. Upper part: experimental setup for grating inscription. Lower part: atomic force microscope surface profile of an optically inscribed grating in a poly(DR13A) copolymer. Reprinted from ref 138. Copyright 1996 American Chemical Society.

The effect of different structures of azo chromophores linked to a polyacrylate or a polymethacrylate backbone has been investigated by Barrett et al.,[138] who compared in equivalent irradiation conditions the diffraction efficiency of different azo polymers whose structures are shown in Figures 5 and 13.

For these three polymers which are structurally similar, the diffraction efficiency varies in the order poly(DR13A) > poly(DR1A) > poly(MEA); i.e., the

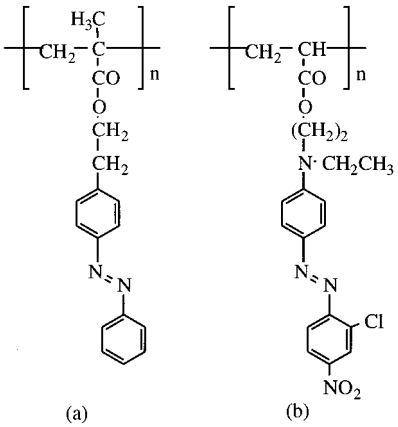

Figure 13. Structures of poly(MEA) (a) and poly(DR13A) (b).

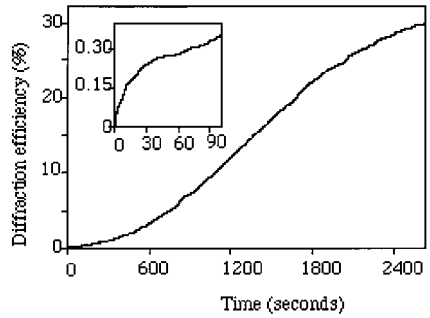

Figure 14. Diffraction efficiency as a function of time under a mixed recording condition (both beams are polarized at 45° with respect to s-polarization). The inset shows the initial stages of the grating formation. Reprinted with permission from ref 141. Copyright 1996 American Institute of Physics.

most bulky azo group induces the highest efficiency.[138] PMMA doped with DR1 also gives surface gratings, but with a much lower efficiency.[139,140]

Bulk properties of the polymer matrix also have an influence on the surface grating formation.[138] Barrett et al. compared poly(DR1A) with copolymers of DR1A with MMA and found similar results, whatever the azo content was, but they also found that compatible blends of poly(DR1A) and PMMA were not suitable for any surface grating formation, even for low PMMA content, and this was attributed to the high molecular weight of PMMA used for blending (MW > 300 000). These authors established an upper experimental limit for the molecular weight of PMMA (MW ≈ 25 000) beyond which only birefringence gratings were obtained.[138] This observation will strengthen models based on mass transport.

The influence of the polarization of both writing beams on the diffraction efficiency is an important observation which is not completely understood. Tripathy et al.[134] have shown that when both writing beams are p-polarized (polarization parallel with the incidence plane), diffraction efficiency is larger than when both beams are s-polarized (polarization perpendicular to the incidence plane).[134] More precisely, the maximum efficiency (27%) and the maximum surface modulation (360 nm, for an initial thickness of 800 nm) are observed when both beams are polarized at 45° with respect to s-polarization.[141] Figure 14 shows the dynamics of the increase of diffraction efficiency in these polarization conditions, for a laser intensity of 55 mW·cm^{-2}. This figure puts into evidence the two distinct processes discussed above: a fast increase during the first 60 s, which is due to birefringence, and a slow and large increase during almost 1 h, due to the surface relief.

It has been observed by several authors[132,135] that illuminated regions of the grating correspond to pits and dark regions to peaks of the surface, except in the case of a side-chain liquid crystalline polyester of low T_g where the opposite result was obtained.[143] More surprising is the fact that irradiation of the film with a polarization grating (see section II) resulting from the interference of two orthogonal circularly polarized beams also creates the largest surface modulation (>350 nm) although the total intensity across the film is constant in this case.[141] Such a result has been confirmed by three other groups.[142−146] Very recently, Ramanujam et al. have demonstrated that it is possible to obtain surface gratings in an azobenzene side-chain polyester (T_g = 63 °C) after irradiation by the single pulse of a Q-switch frequency-doubled Nd^{3+}:YAG laser (532 nm, 5−7 ns duration, energy of 10 mJ).[147] After exposure, AFM investigations reveal the presence of a surface relief grating with a surface modulation greater than 400 nm for a spatial frequency of 160 lines·mm^{-1}. In this case, the depth modulation was concomitant with a refractive index modulation, both reaching a steady-state value less than 10 s after the end of the pulse, so it appears that, at least in this low-T_g polymer, one pumping cycle alone per azo derivative is enough to induce birefringence and surface relief.

Surface relief gratings have generally been registered on azo polymers, but they have also been inscribed on azo-hybrid gels.[148] In this case, the gratings were obtained immediately after the gel film was spin-coated, at a stage where the condensation degree of the gel is low enough to have a weakly cross-linked network which allows volume and surface deformations.

B. Models

Since the first observations, it was recognized by different authors that the mechanism at the origin of surface relief gratings was neither a swelling due to light absorption nor an ablation process in the regions of high intensity.[131−134] The process is also connected with the photoisomerization process of azobenzene derivatives. All the models proposed so far agree with the need of a mass transport well below T_g. The first model was proposed by Barrett et al.[138] and based on the internal pressure created by the isomerization reaction. The idea is that the isomerization process involves creation of a supplementary free volume in going from trans to cis, and that this creation leads to pressure gradients above the yield point of the polymer; the resulting viscoelastic flow then leads to pressure-driven mass transport to form surface profile gratings. A rough estimate of the internal pressure for poly(DR1A) is 2.5×10^7 Pa, which is comparable to the yield point for these polymers estimated as 2×10^7 Pa, so with stress above the yield point in the irradiated regions,

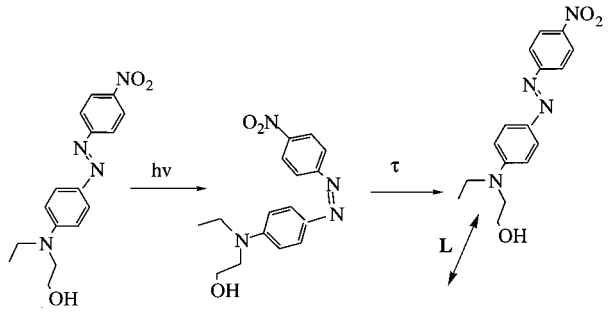

Figure 15. Photoinduced isomerization-induced caterpillar-like motion of the DR1 molecule. After one trans → cis → trans cycle, the DR1 molecule has undergone translation diffusion by an average amount, *L*. Reprinted with permission from ref 139. Copyright 1998 IOP Publishing Limited.

viscoelastic flow results.[138] In a more quantitative approach based on fundamental hydrodynamic theory, Barrett et al.[145] used Navier–Stokes equations for laminar flow of a viscous fluid which relate velocity components to pressure gradients in the polymer film. Considering that the isomerization reaction was the origin of the internal pressure gradients, a specific model was developed which is able to yield an expression relating the time evolution of the surface gratings to experimental parameters, such as light intensity, irradiation geometry, film thickness, and molecular weight of the polymer, and the predictions agree well with the experimental results. However, the influence of the polarization of both writing beams is not completely predicted. The largest efficiency obtained with two orthogonal circularly polarized beams is explained as follows: such beams create interference fringes of constant intensity, but which represent alternating regions of linearly polarized light (which creates selective isomerization) and of elliptically polarized light (which creates unselective isomerization). Thus, this interference creates alternating regions of high (elliptical) and low (linear) isomerization. Similarly, the interference of two linearly polarized beams creates alternating regions of low (linear, bright fringe) and no (destructive interference, dark fringe) isomerization. The presence of a pressure gradient is effective in both cases, but the effect of this gradient will be less in the latter case, in agreement with the experimental observations. However, this model cannot explain the difference in efficiency between the interference of two s-polarized beams and two p-polarized beams. This difference suggests that there is another (perhaps dipolar) force involved in addition to isomerization pressure.

On the basis of this last difference in efficiency, Nunzi et al.[139,140] built a molecular model based on an anisotropic translational diffusion of photochromes in a direction which is parallel to the polarization of the writing beams. The essential feature of their model is that the azo dye molecule undergo a 1D-random walk along the excitation direction, this walk being called caterpillar-like motion (Figure 15).

Although simple, this microscopic model accounts quantitatively for the essential features of surface relief gratings induced by linearly polarized light. It is particularly efficient to explain the difference between s- and p-polarization, as s-polarization essentially tends to move molecules in a direction which is parallel to the fringes. However, this model is inappropriate to explain surface gratings produced by a polarization hologram. A more sophisticated model was developed by Pedersen et al.:[149,150] this model is based on a mean field theory which was first developed to describe PIA (see section II) in liquid crystal polymers,[149] and extended to describe the formation of surface relief gratings.[150] The essential point of this theory is that a chromophore is subject to an ordering mean field potential due to all other chromophores, and hence a chromophore contained in a given volume will tend to align along the director, i.e., the preferred molecular orientation of the volume. The mean field potential model considers intrinsically the intermolecular cooperativity which is needed to explain global mass transport. In this model, the driving force is not trans–cis photoisomerization by itself, but the orientational order, the molecules tending to migrate into domains having a higher *S* order parameter (see section II.A). This theory is also able to explain polarization effects.[150]

Another model was proposed by Kumar et al.[151,152] which stresses the importance of the film surface in the mechanism. According to these authors,[151] forces leading to migration of polymer chains are attributed to molecular dipoles interacting with the gradient of the electric field present in the polymer material. For s-polarized beams, the gradient of the electric field is zero in a direction perpendicular to the fringes, so there is no net force in this direction. Why do only azo polymers form surface relief gratings under this gradient? Because, in such polymers, there is a "light-induced plasticization" of the polymer surface due to trans → cis → trans photoisomerization which allows the motion of the polymer chains.[151] A detailed experimental study has been recently reported[152] which shows that the grating formation process is strongly dependent on the nature of the surface. Indeed, restriction of the surface of the azobenzene polymer film through the deposition of ultrathin layers of transparent polyelectrolytes dramatically decreases the relief grating formation. Barrett et al.[145] also pointed out that their model, which is a volume process, also exhibits strong similarity to a surface process since the velocity components in the film scale with the cube of layer height, which means that the flow of material essentially occurs at the surface of the film. In a recent study, Lagugné Labarthet et al.[144] used a modern Raman confocal microspectrometer, and by analyzing the resonance-enhanced polarized Raman spectra recorded on optically inscribed surface relief gratings in an azo polymer (poly(DR1M-*co*-MMA)), they have obtained for the first time new information about the second (T_2) and fourth (T_4) order parameters of the chromophore orientation function. The information entropy theory used to build the distribution functions $f(\theta)$ from T_2 and T_4 order parameters confirms the important photoinduced orientation in a direction perpendicular to the polarization of the incoming light, but with very broad distribution functions even

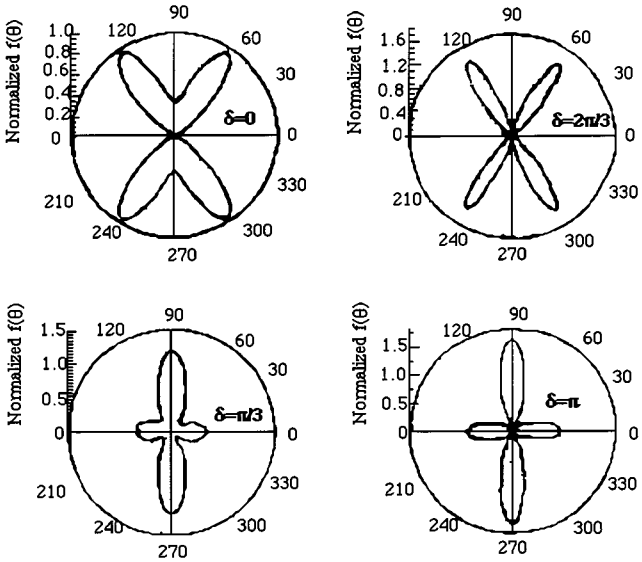

Figure 16. Polar representations of the normalized $f(\theta)$ distribution functions in four distinct regions of the grating surface ($\delta = 0$, $\pi/3$, $2\pi/3$, and π, respectively). Adapted from ref 144.

in the bottom of the gratings. They concluded that the primary orientational order generated by the angle-dependent absorption of light acts as an initializing force. This initial order is then strongly perturbed by the presence of strong pressure gradients as suggested by Barrett et al.[145] Very different distribution profiles at the top and at the bottom of the surface relief (Figure 16) are thus created.

The same authors have recently studied[153] the dynamics of the diffraction efficiency, birefringence, and surface relief modulation on functionalized azo polymer films of poly(DR1M-*co*-MMA) with a 12% mole fraction of DR1M, using parallel and perpendicular linearly polarized pump beams under low irradiances and different polarization configurations for the probe laser. The experimental curves were interpreted by a phenomenological model including a phase grating, a surface relief grating, and a dephasing parameter between both gratings. Numerical calculations allow them to extract the time variations of the birefringence and of the surface modulation and to compare the various efficiencies of writing polarization configurations. Finally, the observed surface profile maxima, which coincide with the maxima of the incident light intensity pattern, seem more consistent with the mean field theory.

C. Applications

Approaches to the unique application possibilities of surface relief gratings have only been recently explored.[154−156] Such gratings could be considered for applications such as holographic storage, optical filters, and resonant couplers. For example, subwavelength gratings could be made by this approach, which could be used in the making of wave plates and antireflection surfaces for the visible. Rochon et al. have made selective wavelength light couplers for slab waveguides by this process.[154,156] The major advantages of this process are (1) the easy one-step processing, without any development, (2) large surface modulations, and (3) precisely controlled modulation depth.[152] The new demonstration of recording holograms after a 5 ns exposure opens the door to instant holography, with possible applications in holographic cinematography.[147]

IV. Molecular Second-Order Nonlinear Optical Polarizabilities of Photochromic Molecules

A. Definitions

Comprehensive treatments of the physics of NLO originating from interaction of atoms and molecules with light can be found elsewhere.[157−159] Here, we will simply define the quantities that we will use further. Electric field (E_a), such as an applied dc field or a propagating electromagnetic wave, always induces displacements of the electronic cloud. In an applied oscillatory field, the electrons will oscillate at the applied frequency. At low field strengths, the magnitude of such an induced polarization will be proportional to the applied field. At high field strengths, the polarization is no longer linear. To account for this nonlinearity, it is common to develop the dipole moment μ of the molecule as a power series expansion in the local electric field E_L:

$$\mu = \mu_0 + \alpha E_L + \beta E_L E_L + \gamma E_L E_L E_L + \ldots \quad (7)$$

In this equation, μ_0 is the permanent dipole moment of the molecule, α is the linear polarizability, β is the first hyperpolarizability, and γ is the second hyperpolarizability. α, β, and γ are tensors of ranks 2, 3, and 4, respectively. Symmetry requires that all terms of even order in the electric field of the above equation vanish when the molecule possesses an inversion center. This means that only noncentrosymmetric photochromic molecules will have second-order NLO properties. In a dielectric medium consisting of polarizable molecules, the local electric field at a given molecule differs from the externally applied field due to the sum of the dipole fields of the other molecules. Different models have been developed to express the local field as a function of the externally applied field E_a;[158,160] however, they will not be developed here. In disordered media, it is useful to define a local field factor f such that $E_L = fE_a$. In the limits of spherical cavities and optical frequency, this local field factor f_∞ can be given by the Lorentz−Lorenz local field correction: $f_\infty = (n^2 + 2)/3$, where n^2 is the square of the refractive index.

Molecules possessing the largest β coefficients contain donor and acceptor substituents linked through an intervening π-backbone. Paranitroaniline is a classical model for these push−pull nonsymmetric molecules. Molecular engineering of this kind of structure has been developed during the past 20 years to increase the β values: this has been done by using more potent donating or accepting moieties or increasing the conjugation length between the substituents.[161,162] Photochromic compounds, which are generally π-conjugated systems, have potential NLO properties. As the colored form is more π−conjugated, we may expect a higher β value. The possibility to switch between two different NLO re-

sponses by irradiation of a material having both NLO and photochromic properties is attractive for applications in optical signal processing.

B. Methods of Determination of Molecular Hyperpolarizabilities: Experiments and Calculations

The first experimental method for β measurements of neutral dipolar methods is the electric field induced second harmonic generation (EFISH).[163] This method consists of measuring the light intensity at a frequency twice the fundamental frequency ω of the infrared nanosecond laser generated by a solution submitted to a static electric field, $E°$. In the case where the static electric field is applied along the Z-axis in the laboratory framework, and the polarization of the laser is also along the same axis, the macroscopic polarization $P^{2\omega}$ induced in the solution by the electric field of the incident laser wave E^{ω} is given by:

$$P_Z^{2\omega} = \Gamma E^0 E_Z^{\omega} E_Z^{\omega} \tag{8}$$

where Γ is the macroscopic third-order susceptibility (only one component Γ_{ZZZZ}) which can be related to the molecular first and second molecular hyperpolarizabilities β and γ:

$$\Gamma = N f_{2\omega} f_{\omega}{}^2 f_0 \left(\gamma + \frac{1}{5}\frac{\mu\beta_z}{kT}\right) \tag{9}$$

where $f_{2\omega}$, f_{ω}, and f_0 are the local field factors at frequencies 2ω, ω, and zero, respectively, μ is the ground-state dipole moment, and β_z is the vectorial component of β along the ground-state dipole moment, supposed to be oriented along the z-axis in the molecular framework ($\beta_z = \beta_{zxx} + \beta_{zyy} + \beta_{zzz}$). The above equation shows two contributions to Γ in the parentheses: the first one is coming from second hyperpolarizability γ, the second one, $\mu\beta_z/5kT$, is coming from the orientation of dipoles with the electrostatic field. For usual π-conjugated chromophores, γ is negligible compared with $\mu\beta_z/5kT$. It is worthwhile to note that, as β_z alone intervenes in the above equation, only a combination of tensorial components of β can be obtained by this method. Finally, in the case of a solution containing one solute, A, both solvent and solute being NLO active, the Γ coefficient varies linearly with the mass fraction x_A of solute A:

$$\Gamma = \Gamma_0 + x_A \Gamma_A' \tag{10}$$

where Γ_A' is the macroscopic third-order susceptibility of solute A, from which β can be determined. In the case of photochromes, as it is generally difficult to isolate colorless and colored forms (noted A and B, respectively), one can perform EFISH experiments on the mixture of both forms A and B at the photostationary state, and in this case Γ is written:

$$\Gamma = \Gamma_0 + x_A \Gamma_A' + x_B \Gamma_B' \tag{11}$$

From the third term Γ_B', and provided that x_A, x_B, Γ_0, and Γ_A' are known, the first hyperpolarizability β_B of the unstable colored form can be determined.

A second experimental method, hyper-Rayleigh scattering (HRS),[164,165] allows β measurements for nondipolar and/or ionic molecules, which are out of reach of the standard EFISH. In this method, a possible experimental arrangement is the following: the fundamental beam of a Nd^{3+}:YAG laser is focused into the solution contained in a parallelepipedic quartz cell presenting five polished windows so as to allow for simultaneous longitudinal illumination and transverse collection of the scattered emission at 2ω. The intensity of the scattered light $I_{2\omega}$ is proportional to the square of the incident intensity and can be written as

$$I_{2\omega} = g(N_{\text{solvent}}\langle\beta^2_{IJK_{\text{solvent}}}\rangle + N_{\text{solute}}\langle\beta^2_{IJK_{\text{solute}}}\rangle)I_{\omega}^2 \tag{12}$$

where N_{solvent} and N_{solute} are the densities of solvent and solute molecules, respectively, $\langle\beta^2_{IJK}\rangle$ is the mean value of the square of some components of the hyperpolarizability tensor in the laboratory framework, and g is a constant value depending on experimental conditions. For example, in a configuration where the fundamental beam is polarized along Z (vertical axis), the harmonic signal also being detected along Z, the above equation reduces to[165]

$$I_Z^{2\omega} = gN\langle\beta^2_{ZZZ}\rangle I_{\omega}^2 \tag{13}$$

In a similar configuration, but with an analyzer at 2ω along X, the detected harmonic intensity is given by

$$I_X^{2\omega} = gN\langle\beta^2_{XZZ}\rangle I_{\omega}^2 \tag{14}$$

The averaged $\langle\beta^2\rangle$ value of the rank-6 tensor $\beta \otimes \beta$ may be expressed in general as linear combinations of polynomial expressions depending on β_{ijk}, the tensor components in the molecular framework. These expressions can be found in the literature; we will simply point out the possibility to obtain by this method different independent tensor components of β, which is not possible by EFISH. Finally, this method can also be applied to a mixture of two species, A and B (for example, the two isomers of a photochrome); in such a case, eq 12 transforms into

$$I_{2\omega} = g(N_{\text{solvent}}\langle\beta^2_{IJK_{\text{solvent}}}\rangle + N_A\langle\beta^2_{IJK_A}\rangle + N_B\langle\beta^2_{IJK_B}\rangle)I_{\omega}^2 \tag{15}$$

During the past decade, theoretical calculations of hyperpolarizabilities[161,166] have been performed to help synthetic chemists in designing optimum NLO structures. Although it is not yet possible to perform extremely accurate calculations, it is now possible to predict the influence of structural changes on the NLO coefficients. In the case of photochromes, theoretical calculations may be very useful for predicting β values of thermally unstable colored forms. The theoretical methods generally employed to calculate molecular hyperpolarizabilities are of two types, those in which the electric field is explicitly included

in the Hamiltonian, frequently labeled as *finite field (FF)*, and those which use standard time dependent perturbation theory, labeled the *sum over states (SOS)* method.

The basis of the FF method is the following. According to eq 7, it is clear that the second partial derivative of the dipole moment with respect to the field, evaluated at zero field, gives the first hyperpolarizability:

$$\beta_{ijk} = \frac{1}{2}\frac{\partial^2 \mu_i}{\partial E_j\, \partial E_k}\bigg|_{E=0} \tag{16}$$

An alternative formulation consists of examining the molecular energy expansion, rather than the previous dipole expansion, with respect to the field:

$$\beta_{ijk} = \frac{1}{2}\frac{\partial^2 \mu_i}{\partial E_j\, \partial E_k} = \frac{1}{2}\frac{\partial^2}{\partial E_j\, \partial E_k}\left(-\frac{\partial W}{\partial E_i}\right) = -\frac{1}{2}\frac{\partial^3 W}{\partial E_i\, \partial E_j\, \partial E_k}\bigg|_{E=0} \tag{17}$$

This method is only valid in the static field limit (zero frequency), and this is a weakness. However, recent advances of a derived procedure (coupled perturbed Hartree−Fock) permit the frequency dependence of hyperpolarizabilities to be computed.[161] The FF method using ab initio model Hamiltonians with correlation corrections is the ultimate procedure to obtain accurate β values, but requires high-level computational resources and long computer times and sometimes gives results whose accuracy drastically depends on the choice of basis functions. For these reasons, semiempirical Hamiltonians have been more extensively used for large push−pull molecules. More precisely, the MNDO (modified neglect of diatomic differential overlap) semiempirical algorithm and the associated parametrizations of AM-1 and PM-3 have been extensively applied to NLO calculations, all the more as they are readily available in the popular MOPAC software package.[167]

The SOS perturbation theory expression (eq 18) for the hyperpolarizability shows that one needs dipole matrix elements between ground and excited states,

$$\beta_{ijk}(-2\omega;\omega,\omega) = \frac{-e^3\pi^2}{h^2}\sum_{n'}\sum_{n}\Bigg\{[\langle ijk\rangle + \langle ikj\rangle] \times \left(\frac{1}{(\omega_{n'}+2\omega)(\omega_n+\omega)} + \frac{1}{(\omega_{n'}-2\omega)(\omega_n-\omega)}\right) + [\langle jki\rangle + \langle kji\rangle]\left(\frac{1}{(\omega_{n'}+\omega)(\omega_n+2\omega)} + \frac{1}{(\omega_{n'}-\omega)(\omega_n-2\omega)}\right) + [\langle kij\rangle + \langle jik\rangle] \times \left(\frac{1}{(\omega_{n'}+\omega)(\omega_n+\omega)} + \frac{1}{(\omega_{n'}-\omega)(\omega_n-\omega)}\right)\Bigg\} \tag{18}$$

$$\langle ijk\rangle = \langle 0|r_i|n'\rangle\langle n'|r_j|n\rangle\langle n|r_k|0\rangle$$

together with excitation energies and excited-state dipole moments to compute β.[168−170] $-e^3\langle ijk\rangle$ represents the product of three transition dipole moments along coordinates i, j, and k, between the ground state $|0\rangle$ and the excited state $|n'\rangle$, between the excited state $|n'\rangle$ and another excited state $|n\rangle$, and finally between the excited state $|n\rangle$ and the ground state. For example, this method has been applied for paranitroaniline by mixing of 60 excited states.[171] By varying the number of excited states, it has been shown that the value of β rapidly converges below approximately 50 excited states.[172] The most widespread Hamiltonian used for this kind of computation is the CNDO/S (completely neglected differential overlap/spectroscopy) or the CNDOVSB,[172] which is a CNDO/S Hamiltonian adjusted to reproduce optical and dipolar data for six molecules with high β values. It is worthwhile to note that the laser frequency ω is an input parameter in the SOS formulation; therefore, first hyperpolarizabilities are computed for some given frequency, and the dispersive character of β can be easily computed. For linear molecules with a large charge transfer in the x direction, eq 18 simplifies into the *two-level approximation*

$$\beta_{xxx}(-2\omega;\omega,\omega) = \frac{6\pi^2}{h^2}\mu_{01}^2\Delta\mu\left(\frac{\omega_1^2}{(\omega_1^2-4\omega^2)(\omega_1^2-\omega^2)}\right) \tag{19}$$

Here, $\hbar\omega$ is the energy of the laser photon, $\hbar\omega_1$ and μ_{01} are the energy difference and the transition dipole moment of the transition from the ground state to the first excited state, respectively, $\Delta\mu$ is the difference in dipole moments between the ground state and first excited state. This equation is often used to determine hyperpolarizability at zero frequency β_0 from experimental values of β, according to

$$\beta_{xxx}(-2\omega;\omega,\omega) = \beta_0 F(\omega,\omega_1) \tag{20}$$

with $\beta_0 = (6\pi^2/h^2\omega_1^2)\mu_{01}^2\Delta\mu$ and the dispersion factor $F(\omega,\omega_1)$ given by

$$F(\omega,\omega_1) = \frac{\omega_1^4}{(\omega_1^2-4\omega^2)(\omega_1^2-\omega^2)} \tag{21}$$

The values of β_0 determined in this way are directly comparable with the values obtained by the FF method. Furthermore, because of the dispersion factor, only values of β_0 of different molecules can be compared.

C. Influence of Photochromism on Molecular Hyperpolarizabilities

Molecular hyperpolarizabilities of the two isomers of different photochromes are presented in Table 1. DR1 is probably the most studied photochrome due to its very interesting NLO properties in polymers as we describe below.[40] The first hyperpolarizability of the trans isomer has already been determined by the EFISH technique,[173−175] but due to the fast back thermal reaction, the cis isomer has not been investigated experimentally. The spiropyran/photomero-

Table 1. Dipole Moments[a] and First Hyperpolarizabilities[b] of Photochromes

Photochrome (most stable or colourless form)	Photochrome (coloured form)	Method [(b)]	Ref.
Trans Disperse Red One 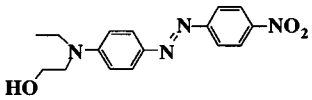 μ = 8.6 D; β = 44.6. 10^{-30} esu	Cis Disperse Red One 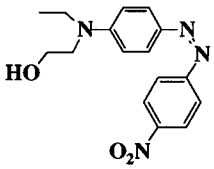 μ = 6.3 D; β = 8.4. 10^{-30} esu	AM1/FF	40
Spiropyran 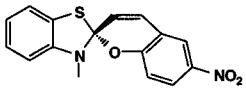 μ = 7.5 D; β = 1.9. 10^{-30} esu	Photomerocyanine 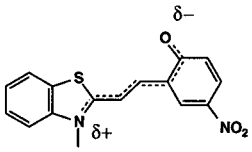 μ = 13.6 D; β = -40. 10^{-30} esu	AM1/FF	177
Furylfulgide Aberchrome 540® 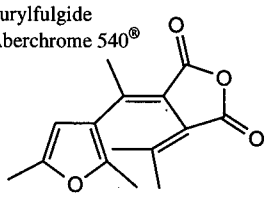 μ = 7.2 D; $\beta\mu$ = 6.6. 10^{-48} esu	Dihydrobenzofurane derivative 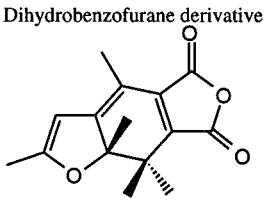 μ = 6.6 D; $\beta\mu$ = 91. 10^{-48} esu	EFISH at 1907 nm	15
Diarylethene (open form) 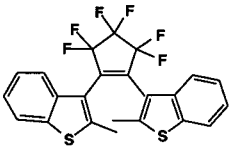 $\beta\mu$ = 13. 10^{-48} esu	Diarylethene (closed form) 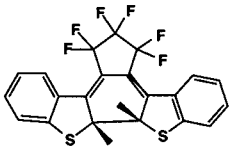 $\beta\mu$ = 55. 10^{-48} esu	EFISH at 1907 nm	15 179
Diaryethene push-pull (open form) 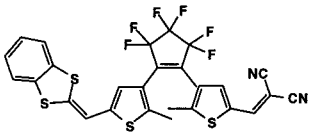 $\beta\mu$ = 260. 10^{-48} esu	Diaryethene push-pull (closed form) 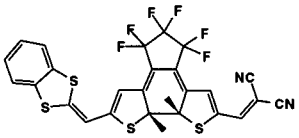 $\beta\mu$ = 1100. 10^{-48} esu	EFISH at 1064 nm	180
N-salicylidene-4-bromoaniline (yellow, stable) 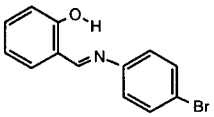 μ = 2.9 D; β = 2.3. 10^{-30} esu	(red, unstable) 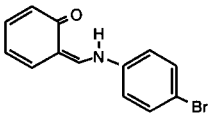 μ = 2.7 D; β = 1.3. 10^{-30} esu	AM1/FF	181

[a] All dipole moments given in this table have been calculated with the AM1/FF method. [b] The method of determination of β is given in the third column. The values obtained by the AM1/FF method are β_0 values. All values are the modulus of the vectorial part of β projected along the direction of the ground-state dipole moment.

cyanine group has also been investigated in detail in polymers and in solutions as well, and the NLO properties have already been described.[176,177] More recently, Atassi et al. have shown that it was possible to observe NLO response with a furylfulgide system,[178,179] and Lehn et al.[180] have shown that some diarylethene compounds can switch photochemically between a low and a high level of NLO response. The first two systems are thermally reversible (on a second time scale for *cis*-DR1 in PMMA[40] and on a day time scale for photomerocyanine in PMMA[177]). On the contrary, the colored forms of the last two systems are thermally stable, but they can be reversed to the colorless forms by visible light irradiation.

The products $\mu\beta$ of furylfulgide and diarylethene in their open and closed forms have been determined experimentally by the EFISH technique, in a mixture of both forms.[15] The main conclusion of these data is the large increase of β in going from a colorless to a colored form of a photochrome: this is true for spiropyran/photomerocyanine, but also for fulgides and diarylethenes. *trans*-DR1 has a larger β and a larger μ than *cis*-DR1, the same holds for photomerocyanine compared to spiropyran, but furylfulgides (and probably diarylethenes) show no significant change in μ upon irradiation. In this table are also included the β values of both isomers of an anil compound, *N*-salicylidene-4-bromoaniline, which will be detailed further for its NLO switching properties in the crystalline state.[181]

Recently, another photochromic system based on nitrobenzylpyridine (NBP) derivatives has been proposed for its potential in switching the second harmonic generation efficiency.[182] The photochromic reaction, given below, implies the change from a colorless "CH" form to a deep blue "NH" form. The mechanism of the process (Figure 17) involves a proton transfer in two steps, through an intermediate "OH" form. The lifetime of the colored "NH" form varies between the millisecond range in solution to several days in polymers.

To stimulate both colorless CH forms and colored NH forms, Lehn and co-workers have synthesized

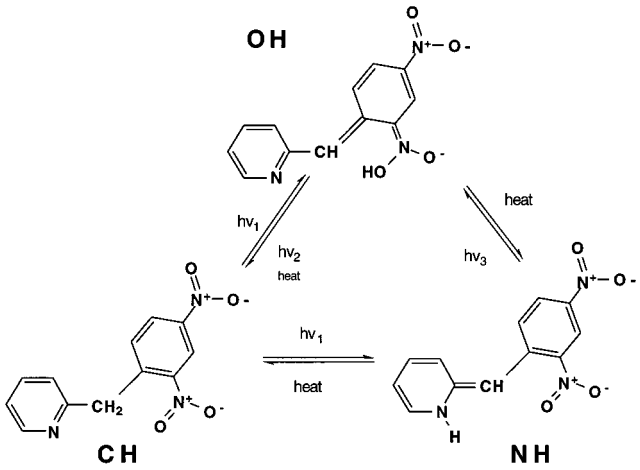

Figure 17. Photochemical and thermal interconversion processes of CH, OH, and NH tautomers of dinitrobenzylpyridine (after ref 182).

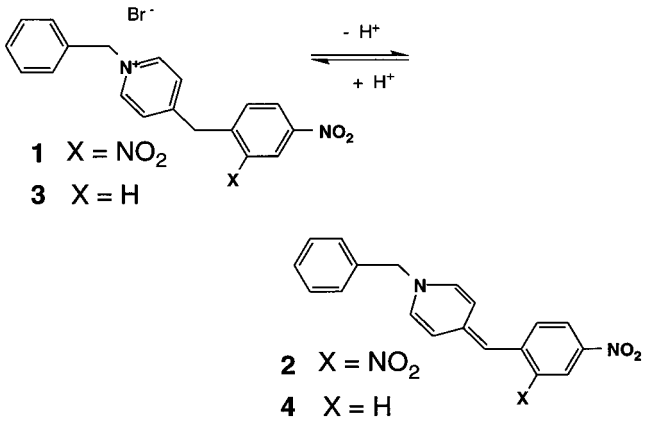

Figure 18. Model nitrobenzylpyridine derivatives (after ref 182).

Table 2. Wavelength of Maximum Absorption λ_{max} (nm), First Hyperpolarizabilities β (10^{-30} esu), and Static Hyperoplarizabilities β_0 Calculated Using the Two-Level Model (10^{-30} esu) (Adapted from Reference 182)

compd	λ_{max}	β	β_0
1	254	2 ± 1	1
2	582	450 ± 5	62
3	262	5 ± 2	3
4	548	1170 ± 100	52

NBP derivatives quaternized by a benzyl group, which can be easily deprotonated to give a stable conjugated form, which is an ideal model of the NH form (Figure 18).

The hyperpolarizability coefficients of these model compounds, determined by the HRS method, are given in Table 2. From this table, it is obvious that the β_0 values of the blue-colored neutral forms **2** and **4** are much higher than those of the colorless CH forms **1** and **3**. Although the error in the measured hyperpolarizabilities of compounds **1** and **3** is large, the order of magnitude of β is comparable to that of nitrobenzene, in agreement with the similarity of their π-systems. Conversely, compounds **2** and **4** have extended π-conjugation, which is accompanied by higher β values. It was concluded that NBP derivatives have potential for optical modulation of the hyperpolarizability and thus for modulating the second harmonic generation efficiency of NLO devices.[182]

V. Poling of Photochromic Materials for Second-Order Nonlinear Optics

A. General Presentation

There have been a tremendous number of push–pull stilbene and azobenzene derivatives studied in the field of second-order NLO. Reviewing all these would require a whole paper, and the reader can refer to some large reviews about NLO organics written in the past years.[160−162] However, in most cases, the photochromic feature of these molecules was not exploited. For a long time, any kind of reactivity has been usually avoided in optical systems.

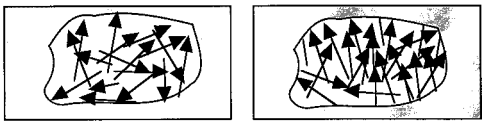

Figure 19. Centrosymmetric (a; $\chi^{(2)} = 0$) and noncentrosymmetric (b; $\chi^{(2)} \neq 0$) media. Arrows represent the dipole moments of molecules.

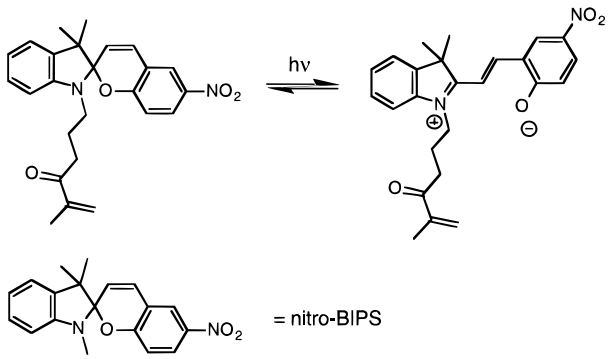

Figure 20. Light-induced activation of second-order NLO properties based on aggregation of photomerocyanine (right). This product is obtained from photochromic nitro-BIPS-type spiropyran (left) (after ref 183).

In second-order NLO, molecules with high quadratic hyperpolarizability (β) and, on a macroscopic scale, materials with high nonlinear susceptibility ($\chi^{(2)}$) are targeted. β and $\chi^{(2)}$ are responsible for NLO efficiency. Both are third-order tensors, and noncentrosymmetry (respectively on microscopic and macroscopic scales) is necessary to get nonzero values. Since $\chi^{(2)}$ is a geometry-sensitive "average of β" over all the molecules contained in a volume unit (eq 22), molecules have to be gathered in a noncentrosymmetric (or acentric) fashion (Figure 19).

$$\chi^{(2)} = \frac{\sum \beta}{V} \tag{22}$$

As pointed out in section IV, some photochromes are good candidates for NLO properties because of their significant dipolar structure and extended π conjugation. DR1 (Table 1) is among the most studied molecules for NLO, since its push−pull structure yields high polarizability.[173−175] In the following, two processes both based on optical pumping which create noncentrosymmetric structures from naturally amorphous and isotropic media are presented.

The first example combining photochromism and NLO is probably the threadlike structure of photomerocyanine reported by Meredith, Krongauz, and Williams.[183] Formation of globules based on crystalline particles of 40 nm size occurs under a dc electric field during irradiation of spiropyran units deposited on a glass plate (Figure 20). Aggregation of highly dipolar photomerocyanine under a dc electric field is responsible for a noncentrosymmetric ordering, causing the medium to exhibit NLO effects. Related photomerocyanine compounds in the liquid crystalline phase were further studied,[184−186] and $\chi^{(2)}$ values as high as 2×10^{-9} esu (ca. 1 pm·V^{-1}) were observed. Blends including push−pull molecules such as 4-(dimethylamino)-4′-nitrostilbene showed enhanced NLO properties.

B. Photoassisted Poling (PAP)

1. Principle

The most widely employed method (Figure 21) to obtain a poled structure in a polymer is to heat a thin film up to its glass transition temperature (T_g), to apply a high dc voltage, and finally to cool the sample to room temperature with the voltage still on.[187] A static field (E_0) of a few MV·cm^{-1} is applied across the sample, either by putting the sample between two electrodes or by corona discharge. This process is called thermally assisted poling (TAP).

When the material is photochromic, a process based on PIA (see section II) can be employed. However, compared to PIA, the application of a dc electric field (poling field) in addition to the pumping beam is necessary, since the symmetry of the latter does not allow the creation of a noncentrosymmetric order. The experimental setup commonly used is shown in Figure 21. This configuration allows the application of optical pumping and a subsequent and/or simultaneous dc electric field. In appropriate materials, the so-called PAP process allows to create a non centrosymmetric order even below the T_g to be created. Compared to TAP, heat is replaced by optical pumping, which enables the molecules to get into motion.

The fundamental mechanism of PAP has been described mainly by Dumont and Sekkat.[26,28,72,81,188−190] It is based on the three processes responsible for PIA (angular hole burning, angular redistribution, and rotational diffusion). However, the random and isotropic feature of angular redistribution in PIA is broken by the dc electric field: the torque of this field on the dipole moment of the molecules makes them rotate along the field direction. Angular hole burning is thus enhanced by angular redistribution. In addition, the rotational diffusion, depicted by a Smoluchowski diffusion operator, is influenced by the presence of a dc electric field. Hence, in the case of PAP, the Smoluchowski term $D_X \Delta n_X$ (X = T or C, last term of eqs 1 and 2) is written:[26]

$$D_X\left(\Delta n_X(\Omega) + \frac{1}{kT}\nabla(n_X(\Omega)\,\nabla(U))\right) \tag{23}$$

$$U = -\mu_X\, E_0 \cos\theta \tag{24}$$

μ_X and E_0 are, respectively, the dipole moment of species X and the dc electric field. The other parameters are defined in section II.

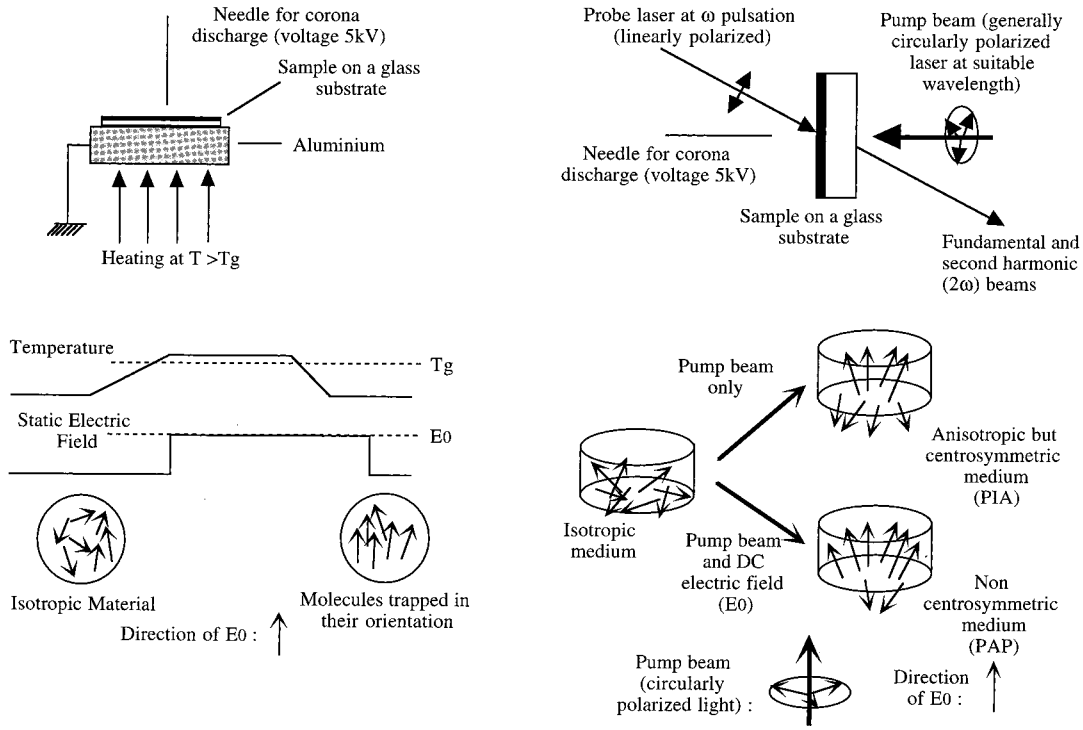

Figure 21. Poling methods for amorphous polymers. Upper left: setup for TAP, which allows heating to the glass transition temperature (T_g) and application of a poling electric field (E_0) by corona discharge. Lower left: time sequence for TAP, showing the application of E_0 when the sample is cooled from T_g to room temperature. Upper right: setup for PAP by the application of E_0 and a pump beam at a suitable wavelength for photochromic reaction. A probe beam (e.g., a Nd^{3+}:YAG nanosecond pulse laser, 1064 nm) allows second harmonic generation (SHG) measurements. Lower right: schematic view of the PAP mechanism compared to that of PIA. In both cases, molecular dipoles line up perpendicular to the pump beam's polarization. E_0 breaks the symmetry between "upward" and "downward" orientations.

Equations 5 and 6 written for PIA are modified as follows:[26]

$$\frac{dT_q}{dt} = -\sum_{q'} \mathrm{Pr}_{qq'} T_{q'} + \frac{1}{\tau_C} \sum_{q'} R^{CT}_{qq'} C_{q'} - q(q+1) D_T \left(T_q + \frac{\mu_T E_0}{kT} \frac{T_{q+1} - T_{q-1}}{2q+1} \right) \quad (25)$$

$$\frac{dC_q}{dt} = -\sum_{q'q''} R^{TC}_{qq'} \mathrm{Pr}_{q'q''} T_{q''} - \frac{1}{\tau_C} C_q - q(q+1) D_C \left(C_q + \frac{\mu_C E_0}{kT} \frac{C_{q+1} - C_{q-1}}{2q+1} \right) \quad (26)$$

The terms $R^{CT}_{qq'}$ and $R^{TC}_{qq'}$ differ in this set of equations from those in eqs 5 and 6. This is due to the presence of a poling torque competing with the isotropic redistribution. In the diffusion term, the torque of the dc electric field on the dipole moment introduces a coupling between $\Delta q = \pm 1$ terms, which describes the creation of noncentrosymmetry.

2. Measurement Techniques

SHG,[191] ATR,[71] and Stark (electroabsorption) spectroscopy[192,193] were employed to evidence PAP. The response of the interaction between an electric field (E_a) and a material can be described by eq 27, where P is the polarization, P_0 is the permanent polarization, $\chi^{(1)}$ is the linear susceptibility, and $\chi^{(2)}$ and $\chi^{(3)}$ are the quadratic and cubic (nonlinear) susceptibilities.

$$P = P_0 + \chi^{(1)} E_a + \chi^{(2)} E_a^2 + \chi^{(3)} E_a^3 + \ldots \quad (27)$$

When E_a is associated with a ω frequency ($E_a = E_{a0} \cos(\omega t)$) electromagnetic wave, one gets a 2ω response (SHG) provided that $\chi^{(2)}$ is not equal to zero (eq 28).[194] Figure 21 shows a crossed-beam setup which allows probing of SHG during PAP.

$$\chi^{(2)} E_a^2 = {}^1/_2\, \chi^{(2)} E_{a0}^2 (1 + \cos(2\omega t)) \quad (28)$$

In ATR, application of a combination of poling dc (E_0) and measuring ac ($E_1 \cos(\Omega t)$) electric fields modifies the angular positions of the Fabry−Perot dips (Figure 3). The shift is related to a small change of the refractive index ($\Delta n = 10^{-5}$). $\Delta n_i(\Omega)$ and $\Delta n_i(2\Omega)$ (with $i = x, y, z$), the Ω and 2Ω modulated signals, are measured and related to the nonlinear susceptibilities, and to the Pockels (r_{iz}) and Kerr (s_{iz}) coefficients (eqs 29 and 30).

$$2\chi^{(2)}_{iiz} = -r_{iz} n_i^4 = 2 n_i \Delta n_i(\Omega) E_1^{-1} \quad (29)$$

$$3\chi^{(3)}_{iizz} = -s_{iz} n_i^4 = 4 n_i \Delta n_i(2\Omega) E_1^{-2} \quad (30)$$

Along the poling direction (z), the refractive index change is given by eq 31.[188]

$$2 n_z \Delta n_z(\Omega) = (2\chi^{(2)}_{333} + 6\chi^{(3)}_{3333} E_0) E_1 \cos(\Omega t) + \frac{3}{2} \chi^{(3)}_{3333} E_1^2 \cos(2\Omega t) + \ldots \quad (31)$$

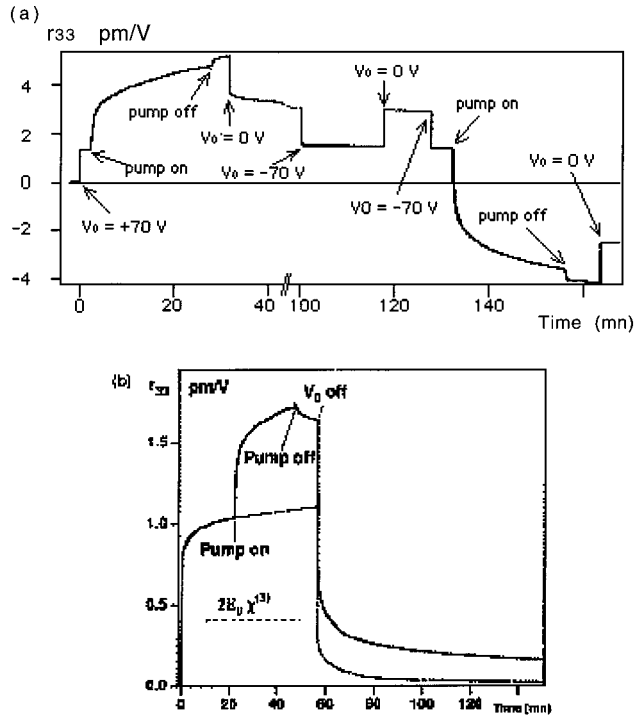

Figure 22. PAP of DR1 polymer films (thickness around 1 μm) monitored by the ATR technique. V_0 is the voltage corresponding to the poling electric field. The pump beam is an argon ion laser (circularly polarized, 488 nm). (a) Poly(DR1M-*co*-MMA) copolymer (pump intensity ca. 30 mW·m^{-2}), after the poling sequence (0−40 min); the effect of a reverse electric field with and without optical pumping is shown (100−170 mn). (b) DR1-doped PMMA (pump intensity ca. 8 mW·cm^{-2}). The dotted line shows the effect of V_0 alone. Both curves show that, though the electric field alone yields an electrooptic signal (r_{33}) due to $\chi^{(3)}$, there is no remnant r_{33}. Reprinted with permission from ref 71. Copyright 1993 Gordon and Breach Publishers.

As written in eq 32, Stark spectroscopy is based on the absorption spectrum change (ΔA) induced by

$$\Delta A(\Omega) = E(\Omega)\,\frac{\Delta\mu S_1}{hc}\nu\,\frac{\partial(A/\nu)}{\partial\nu} \qquad (32)$$

an electric field (of frequency Ω).[193] A is the absorbance, ν the wavenumber, and $\Delta\mu$ the dipole moment change between the ground and excited states.

From measurement of $\Delta\mu$, A, and ΔA, the polar order parameter S_1 is determined. S_1 is connected to the Legendre polynomials and to $\chi^{(2)}$ (eqs 33 and 34).

$$S_1 = \frac{\langle\cos\theta\rangle - \langle\cos^3\theta\rangle}{1 - \langle\cos^2\theta\rangle} \qquad (33)$$

$$\chi^{(2)}_{zxx} \propto \langle\cos\theta\rangle - \langle\cos^3\theta\rangle \qquad (34)$$

3. Examples

The first examples arise from PMMA doped with DR1, and poly(DR1M-*co*-MMA) (Figure 22).[188,189] The initial appearance of the electrooptic signal at the onset of E_0 is due (partly in the case of the doped polymer and totally in the case of the side-chain polymer) to the Kerr effect term in eq 31, which does not require poling. The subsequent increase of the electrooptic signal is the poling process itself that occurs during the trans−cis photoisomerization cycles. It is due to the noncentrosymmetric order created by photoexcitation under a dc electric field. After the dc electric field is switched off, the electrooptic signal is maintained. This evidences the achievement of a poled structure. In the case of the doped polymer, it is worthwhile to note that some chromophores can orient even when optical pumping is not applied; however, there is no remnant poling when the poling field is removed. In terms of the NLO response as well as orientational stability after poling, the side-chain copolymer turned out to be a better material (Figure 22). An electrooptic coefficient r_{33}(eq 29) of 5.7 pm·V^{-1} 40 h after the poling process and a d_{33}[194] of 7−10 pm·V^{-1} measured by SHG 1 h after the poling process [71,195] are reported for the side-chain copolymer. In this polymer, photoisomerization during PAP pulls on the polymer main chain, leading to a stabilizing rearrangement.[196] PAP with a pulsed pump beam was also reported.[197]

PAP was applied in other polymer materials. DR1-doped polystyrene featured properties similar to those of DR1-doped PMMA.[191,198] Polyester with side-chain DR1 was synthesized and oriented by PAP at two different poling fields.[199] The fraction of azo moieties that gets oriented at 70 and 40 V is different, yielding a r_{33} ratio of 1.75. In DR1-doped poly(vinylcarbazole),[198] photoconductivity annihilates the poling field and hinders PAP. This result stresses the absolute necessity of a dc electric field during the process. PAPs of dimethylaminonitroazobenzene in polycarbonate and poly(ethylene-*co*-*N*-hexyl-*N*-(4-methacryloxybutyl)aminonitrostilbene) were reported.[193] By Stark spectroscopy, the authors compare the orientation of the two materials. The results (polar order parameters S_1 of 0.07 for the former vs 0.023 for the latter) stress the influence of the photoisomerization efficiency, which is higher in the azobenzene derivative.

A further photochromic system studied was spiropyran/photomerocyanine (nitro-BIPS, Figure 20) in PMMA.[74,81,101,174,191,200] Compared to DR1, the "unstable" photoisomer (photomerocyanine) is "more stable", and the gap between the dipolar and polarizability properties between the isomers is larger (see section IV). This provides particular interest, since separate contributions of the photoassisted process and spontaneous thermal diffusion process could be evidenced and compared.[101] By analogy to what is observed with mechanical stress, the angular mobility was proved to be dependent on the time sequence of the application of optical pumping and of a dc electric field. The shorter the delay between both, the higher the efficiency.[74,101] In addition, a simultaneous application of both perturbations yields a more efficient orientation than a consecutive one (Figure 23), which evidences a synergistic effect of the dc field and optical pumping.[174] According to these results, the volume created around the photochromic species during photoreaction allows easier rotation, and thus poling of the chromophores. In the case of Aberchrome 540 (Table 1) in PMMA (doped),[175] the photoinduced effect is reported to be less significant compared to thermal diffusion. This is attributed to

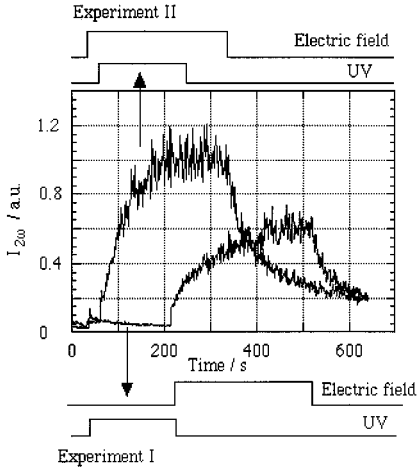

Figure 23. PAP on a spiropyran (nitro-BIPS, Figure 20) doped PMMA film (25% w/w) probed by SHG ($I_{2\omega}$) at 1064 nm, pumping at 355 nm, 10 mW·cm^{-2}. Experiment II (simultaneous poling and pumping) yields a higher SHG signal than experiment I (poling after pumping). Reprinted from ref 177. Copyright 1995 American Chemical Society.

the more globular structure of the colored isomer of Aberchrome 540, which allows this molecule to rotate in the matrix even without photoexcitation.

The poled structure is a metastable state. Hence, the orientational stability of poled polymers is among the main concerns of the last few years. One of the strategies to achieve this is the use of high-T_g polymers, such as polyimides. In fact, below T_g, it is commonly admitted that the time constant (τ) that characterizes the orientation decay (randomization) can be fitted by the Williams−Landel−Ferry equation (WLF; eq 35),[201] an Arrhenius-type law describ-

$$\tau(T) = A \exp\left(-\frac{B}{T_0 - T}\right) \tag{35}$$

ing that the higher the difference between the operating temperature and T_g, the more stable the orientation is expected to be. τ is obtained by a Kohlrausch−Williams−Watts (KWW) or stretched exponential law fit (eq 36).[202]

$$I(t) = I(0) \exp\left(-\frac{t}{\tau}\right)^{\beta} \tag{36}$$

A is a preexponential factor, B is related to the activation energy, and $T_0 = T_g + 50$ (K). $I(t)$ is the NLO response as a function of time, and β characterizes the distribution of sites corresponding to different relaxation time constants in the matrix.

There have been a fast growing number of polyimides for NLO synthesized during the 1990s. Though this paper is not aimed to review all these, it is worth mentioning that progress in synthesis, leading to the appearance of soluble polyimides, enabled easy processing of these polymers for NLO purposes[203−206] and that exceptional orientational stabilities with τ values up to a few centuries [207] encouraged this research. Regarding application of PAP, it should be noted that the process occurs at room temperature in some polyimides despite high rigidity of the matrix.[81,208−211] However, a study comparing donor-embedded polyimides (Figure 7, PI-1 and PI-2) and a side-chain polyimide with flexible tether (PI-3a) showed that PAP occurred at room temperature in PI-3a but not in the other two polymers, though T_g values are rather close for PI-2 and PI-3a: embedding the electron donor group in the main chain hinders poling of the chromophore, and heating to temperatures within 100 °C from T_g is necessary. This evidences the importance of the molecular structure of the building block. However, though successfully performed, PAP at room temperature in PI-3a yields SHG 1−2 orders of magnitude below that obtained by TAP at T_g. In this example, efficient poling requires rotation not only of the NLO chromophore itself but also of the main chain. Coupling between these two kinds of rotation is weak. A different behavior was reported in another polyimide (Figure 24):[211] the efficiency of poling can be enhanced by heating the material, but still remaining below T_g. In this example, the sub-T_g transition (β transition) temperature (T_β) related to local movements of the polymer is a determining factor, and whether PAP is performed below or above T_β is of prime importance for the poling efficiency. Compared to that in poly(DR1M-*co*-MMA), angular redistribution is much slower in DR1−polyimide copolymer, but more efficient after a long optical pumping, and the resulting orientation is more stable.[196]

The efficiency obtained by PAP is as high as in TAP, at least for poly(DR1M-*co*-MMA).[71] In a soluble

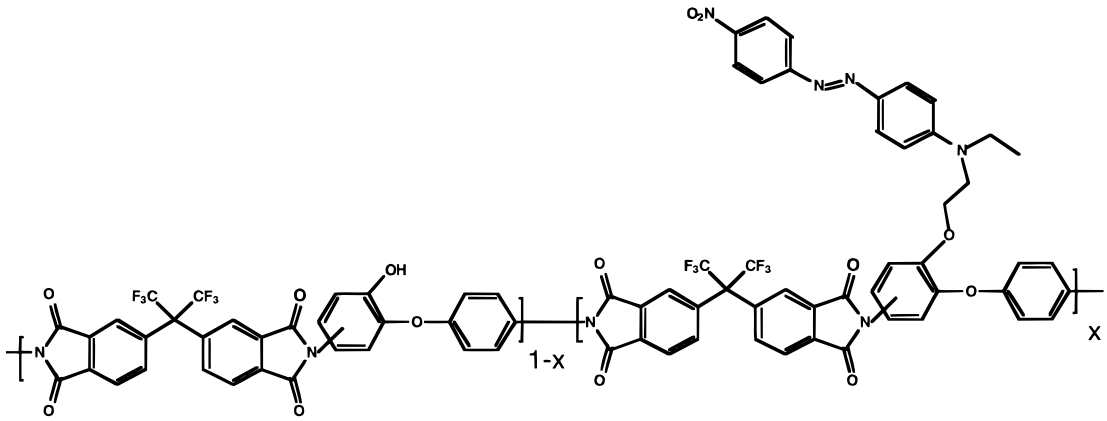

Figure 24. Soluble polyimide with DR1 side chain (T_g = 250 °C for x = 0.31). Reprinted with permission from ref 211. Copyright 1999 Gordon and Breach Publishers.

Table 3. Comparison of NLO Efficiency (d_{33}) and Degradation Ratio (α) According to the Poling Temperature (T_p) for PAP[a]

T_p/°C	25	50	90	120	150	210
d_{33}/pm·V^{-1}	11	17	26	30	47	37
α/%	2.0	1.5	2.2	2.5	2.4	11

[a] Comparison with TAP at 210 °C (last column). The sample is the DR1 side-chain polyimide shown in Figure 24. Reprinted with permission from ref 211. Copyright 1999 Gordon and Breach Publishers.

polyimide with a DR1 side chain (Figure 24), PAP performed at elevated temperature but below T_g (ca. 100 °C below) gave higher d_{33} values than TAP (Table 3).[208,211] This avoids treating the sample at high temperature during poling, and less significant degradation of the chromophore was reported by PAP than TAP.[211] However, it has been shown in DR1-doped PMMA that PAP-poled samples lack orientational stability compared to TAP-poled ones. Stretched exponential analysis gives values of $1/\tau = 1200$ s^{-1} (TAP) and 20 000 s^{-1} (PAP).[212] A complete reorganization of the polymer backbone seems to be impossible at sub-T_g temperatures. Depoling studies by pyroelectric measurements back up these results: depoling occurs at 80, 110, and 140 °C for PAP-poled samples and at 40 and 80 °C for TAP-poled samples.[213]

SHG as high as in TAP-poled samples was reported in PAP-poled liquid crystalline samples containing push−pull azobenzene derivatives.[214] Light-induced polar structures in organic molecular films were also studied by Stark spectroscopy on a Langmuir-type organic molecular film deposited between two electrodes,[192] and by SHG in hybrid materials made by sol−gel methods.[215]

4. Applications

There is a risk of destroying the organic chromophores during TAP, especially in the case of high-T_g polymers. For this reason, PAP, which can be efficiently performed at sub-T_g temperatures, is of particular interest.

Another application of PAP is the patterning of quasi-phase-matched configurations. In dispersive media like polymers, phase mismatch occurs, due to the difference of the refractive index between ω and 2ω. As a consequence, SHG intensity is a sinusoidal function of the propagation length. The half-period is the coherence length (Figure 25). A way to avoid the signal decrease after one coherence length is to create an alternating poling pattern every half-period. PAP may be used for this purpose, since small areas of a material can be accurately selected.

In this field, the combination of photoprocesses and thermal processes provides a technique suitable for building particular dipole orientation ("orientation grating") aimed for waveguide applications.[217] Such a device was realized on a styrene-*co*-anhydride-based polymer with DR1 side chains, by simultaneous application of a laser beam and alternating the electric field while translating (Figure 26). Using such a technique, the full width at half-maximum (fwhm), which characterizes the spatial resolution, was 7 μm for a beam diameter of 1.5 μm. Further potentialities of this poling technique are reviewed by Gerhard-Multhaupt and Bauer-Gogonea.[218]

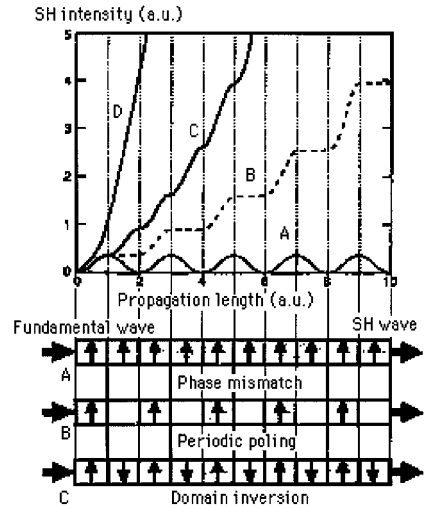

Figure 25. SHG intensity as a function of the propagation length. Between the two "extreme" cases (phase mismatch, A, and phase match, D), periodic poling (B) and domain inversion (C) are intermediate patterns which may be drawn by PAP. One unit along the propagation length corresponds to the coherence length. Reprinted with permission from ref 216. Copyright 1997 CRC Press.

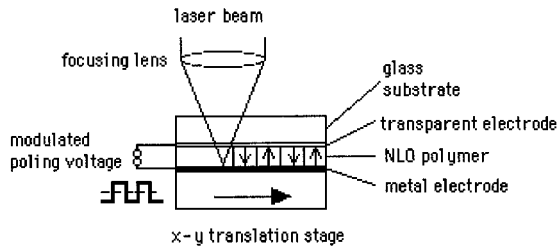

Figure 26. Photothermal poling setup. Poling voltage modulation is synchronized with the translation. Local illumination (He−Ne laser, 2 mW, 543 nm) provides heat to reach T_g. Reprinted with permission from ref 217. Copyright 1994 American Institute of Physics.

C. All-Optical Poling

1. Principle

A monochromatic wave is centrosymmetric and thus cannot induce noncentrosymmetry by itself. Hence, in PAP (see section V.B) based on the excitation of photochromes in their absorption band, superimposition of a dc electric field is needed.

Another way to induce noncentrosymmetry is all-optical poling (AOP). A coherent superposition with the appropriate phase difference of two optical waves, one at the frequency ω and another at 2ω, yields a noncentrosymmetric resultant field, E, by combination of the respective electric fields E_ω and $E_{2\omega}$ (Figure 27).[219−222] In other words, E makes the difference between "upward" and "downward" molecules, and can be differently selected. For a given location, the quadratic susceptibility ($\chi^{(2)}$) is proportional to $\langle E^3 \rangle$, the time average of E^3. A nonzero value of $\langle E^3 \rangle$ breaks centrosymmetry, and thus induces polarity. An induced susceptibility ($\chi^{(2)}_{ind}(z)$ at abscissa z) is created, as expressed in eq 37.[223,224] $\Delta\Phi$

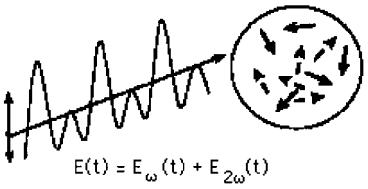

Figure 27. Noncentrosymmetric field E resulting from the combination of E_ω and $E_{2\omega}$. Excitation of a centrosymmetric arrangement of molecules yields a noncentrosymmetric order. Reprinted with permission from ref 226. Copyright 1998 IOP Publishing Ltd.

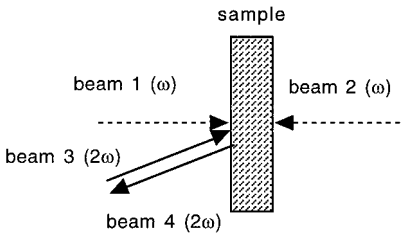

Figure 28. Beam configuration for AOP. During seeding, beam 3 (2ω) is combined with beam 1 (ω, forward configuration) or beam 2 (ω, backward configuration). After seeding, beam 3 is stopped, and SHG (beam 4) is generated due to the polar order created in the sample. Reprinted with permission from ref 219. Copyright 1992 American Physical Society.

and Δk are, respectively, the phase and the wave vector differences between the two beams, and α is the absorption loss coefficient at 2ω (absorption loss at ω is neglected).

$$\chi^{(2)}_{\text{ind}}(z) \propto |E^2_\omega E^*_{2\omega}| \cos(\Delta\Phi + \Delta kz) \exp\left(-\frac{\alpha}{2}z\right) \quad (37)$$

The first examples of AOP were reported on tetrahydrofuran solution of 4-diethylamino-4′-nitrostilbene,[219] and poly(DR1M-*co*-MMA).[220] The experimental configuration to achieve this is shown in Figure 28.[219] During the first step of the process, linearly polarized ω and 2ω beams (respectively beam 1 and beam 3) are applied. This is called the seeding process. Then, beam 3 is stopped, and the achievement of a polar order is evidenced by the generation of beam 4 at 2ω. Forward (beam 1) or backward (beam 2) configurations are possible for the ω beam. The former is reported to lead to more efficient seeding than the latter.

The mechanism is interpreted as a light-induced excitation of chromophores, leading to orientational hole burning and angular redistribution. However, compared to the case of PAP where excitation at only one wavelength is considered, each process involved in AOP is composed of three terms, respectively originating from ω-excitation, 2ω-excitation, and the interference between both.[223−227] The orientation dynamics depends on the value of $|E^2_\omega E_{2\omega}|$, whereas the seeding ratio ($|E_{2\omega}E^2_\omega|$) has to be optimized if one seeks high d_{33} values. The highest values in poly(DR1M-*co*-MMA) were estimated at around 70 pm·V^{-1}.[225]

It has also been demonstrated that, in dispersive materials such as polymers, the periodicity of the field pattern written in the sample corresponds to the coherence length, and phase matching can be achieved by AOP.[223,227] SHG is thus proportional to the square of the optical path length. Other studies concern the use of circularly polarized seeding beams.[228]

2. Photochromes for AOP and Applications

Up to now, only DR1-type photochromes were used in AOP. The comparison between DR1-doped PMMA and the side-chain equivalent, poly(DR1M-*co*-MMA), showed the influence of the rotational diffusion constant on the poling growth rate and on the maximum SHG activity. There is a trade-off between matrix rigidity and photoinduced reorientation efficiency. The higher diffusion in the host−guest polymer compared to the side-chain analogue results in faster growing (3 times), but in a lower value of SHG (2.5 times).[227]

AOP was also reported in rigid polyimides. The influence of the seeding temperature on the maximum d_{33} value as well as on the orientational stability was studied. The d_{33} value ranged from 2.6 pm·V^{-1} (seeding at room temperature)[229] to 6.9 pm·V^{-1} (seeding at 150 °C).[230] Stable patterns (seeding at 150 °C) of optical recording readable by an IR probe were thus written. Seeding rates as well as relaxation rates after seeding are compared between PMMA and polyimide matrixes. As expected, both seeding and relaxation occur faster in PMMA.[231]

PMMA with low absorbing chromophores (DR1 analogue bearing a phosphine oxide instead of a nitro group)[232] exhibits a NLO activity (d_{33} = 8 pm·V^{-1}). Trade-off between NLO efficiency and transparency is an important problem, and such a chromophore is particularly interesting.

This poling method is not limited to photochromes, and can also be applied to molecules which absorb neither ω nor 2ω. Examples are *N*,*N*-diethylnitroaniline side-chain PMMA,[233] and ethyl violet in propanediol[234] and in a hybrid (sol−gel) matrix.[235] Ethyl violet is an octupolar molecule (noncentrosymmetric and nondipolar) with significant quadratic hyperpolarizability.

AOP leads naturally to a phase-matched pattern (see section V.B),[223] which is advantageous for applications. Adding the fact that a wide range of systems such as nonphotochromic, nondipolar molecules as well as rigid polymers can be poled by AOP, it can be considered as a powerful method.

VI. Photoswitching of NLO Properties in Organized Systems and Materials

A. Introduction

The merit of photochromes is that conversion between the two species is chemically reversible, hence enabling photoswitching of various properties between two molecular species.[236] As pointed out in section IV, the two molecular species in a photochromic couple can exhibit different molecular NLO properties. Attempts to extend this property to an organized system (monolayer) and to a material (polymer, crystal) are reviewed in this section.

B. Photoswitching in Polymers

In all examples mentioned herein, polymers were poled thin films.

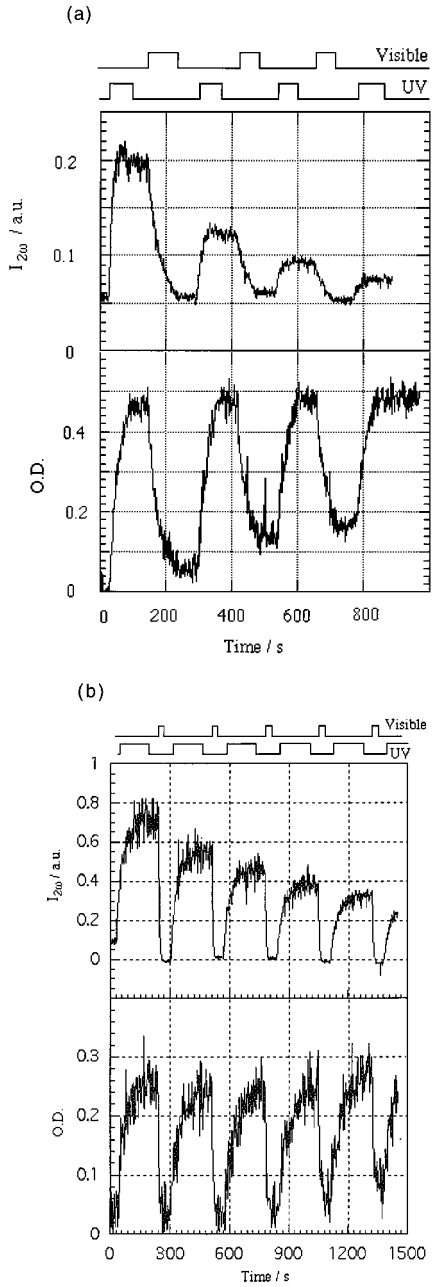

Figure 29. Photoswitching of SHG (upper curve) in a photochrome-doped PMMA thin film (previously poled). UV irradiation is performed at 355 nm and visible irradiation at 514 nm. The optical density (lower curve) is measured within the absorption band of the colored isomer (532 nm) to follow the photoreaction. No electric field is applied during these experiments. (a) spiropyran (nitro-BIPS, Figure 20), 25% w/w, and (b) furylfulgide (Aberchrome 540), 10% w/w. Reprinted from ref 177. Copyright 1995 American Chemical Society.

There is a great enhancement of the hyperpolarizability when spiropyran is switched to photomerocyanine (see section IV). According to the values of β, one could expect an increase of SHG of 3 orders of magnitude if the conversion is complete. A previously poled spiropyran (nitro-BIPS, Figure 20) doped PMMA was photoswitched by UV irradiation, and this resulted in a 10 times increase of the SHG signal (Figure 29).[177] A subsequent visible irradiation within the absorption band of photomerocyanine induced the reverse reaction, and a drop of SHG to almost zero.

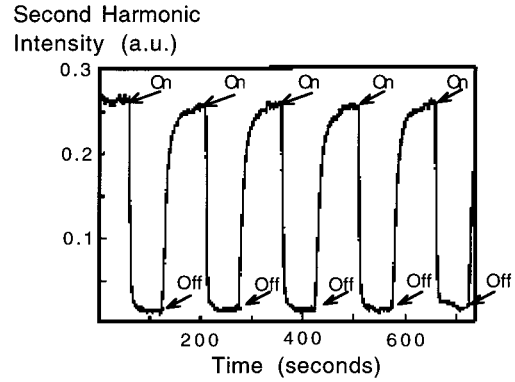

Figure 30. Photoswitching of SHG in PI-2 (Figure 7) under a dc electric field. "On" and "Off" refer to the pump beam (543.5 nm, 8 mW·cm^{-2}). Reprinted with permission from ref 81. Copyright 1998 Optical Society of America.

Despite clear evidence of photoswitching, this system suffers from drawbacks related to the two following reasons: (i) the high-β species is not thermally stable; (ii) the recycling ability of spiropyran is rather low.

Another problem is that switching of the SHG signal is possible only for a limited number of cycles: the higher SHG value reached after UV irradiation decreases with the number of cycles performed. This is interpreted as an effect of disorientation. Indeed, in the absence of a poling field, the chromophores have no reason to recover exactly the same orientation after one isomerization cycle. In the worst cases, the poled order is completely lost after one switching attempt. Usually, this type of disorientation occurs faster in side-chain polymers than in doped ones.[40,237]

The same kind of experiment (Figure 29) was also performed on a furylfulgide (Aberchrome 540, Table 1).[178] The lowering of the higher plateau cannot be avoided, but is somehow slowed. Compared to those in spiropyran, the ring opening and closure reactions need less free volume, so the matrix is less disturbed by the molecular movements. Another advantage of furylfulgide is the thermal stability of the high-β form.

Losing the SHG signal after each cycle can be avoided by applying an external electric field during the switching procedure. There are at least two examples, based on polyimides with a pendant photoisomerizable azobenzene derivative.[81,237] In poled polymers, irradiation in the absorption band of the photoisomerizable entity causes a SHG decay correlated with trans → cis reaction of the azo function, and a recovery to the initial SHG level when left in the dark (Figure 30). Due to the presence of an external electric field, the so-called EFISH signal has to be considered; i.e., not only the difference of β values between the isomers but also that of γ values has to be taken into account. According to Sekkat et al.,[81] the polarization of the pump beam has little influence on the decay. Apart from the SHG switching due to the chemical reaction, this switching process under an external static electric field can be viewed as a competition between photoinduced disorientation and photoassisted poling. An analogous experimental procedure was applied to a DR1-doped PMMA, and gave similar results.[238]

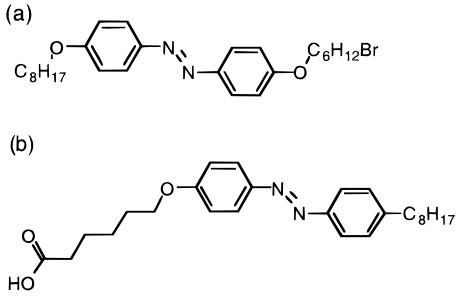

Figure 31. Examples of amphiphile molecules for SHG switching in LB films: (a) 4-(octoxy)-4′-(6-bromohexamethyleneoxy)azobenzene and (b) 4-octyl-4′-(5-carboxypentamethyleneoxy)azobenzene. Reprinted with permission from refs 239 and 240. Copyright 1997 Chemical Society of Japan.

C. Photoswitching in Other Systems

Attempts at all-optical switching of NLO properties have been more successful in monolayered films. Examples from the literature deal with monolayers adsorbed on quartz substrates. The noncentrosymmetry arises from the intrinsic noncentrosymmetry of the interface, and SHG is generated on the layer of the substrate's coating. One example is an almost symmetrical dialkoxyazobenzene.[239] As can be deduced from the molecules' shapes, the cis isomer is expected to be active, whereas the trans isomer is not (Figure 31). Successive short-wavelength (<400 nm) irradiations alternated with long-wavelength (>400 nm) ones make the sample switch from a cis-rich to a trans-rich mixture. Another example is a LB film of 4-octyl-4′-(5-carboxypentamethyleneoxy)-azobenzene, which exhibits the same switching property (Figure 31).[240]

One last example is taken from crystalline photochromes. 4-Bromosalicylideneaniline combines the following characteristics: it is photochromic in the bulk crystal, and the crystal is noncentrosymmetric.[181] In such a crystal, reversible SHG intensity switching originates from the proton transfer between the OH and NH forms. However, the modulation is rather weak (10% at a 1907 nm fundamental wavelength, and 60% at 1064 nm, but in the latter case, absorption of the second harmonic by the NH form contributes artificially to the SHG intensity change).

D. Potential Applications

Obtaining an efficient NLO switching material is not easy, since reversibility of the molecular reaction does not always imply the reversibility of macroscopic physical properties. Further studies should concern the photochromic molecule itself as well as the type of material used. On a molecular scale, a photochrome exhibiting large differences between the two properties of the two forms and efficient conversion should be examined. Concerning the material, there is a subtle trade-off between the rigidity so that disorientation can be avoided, and flexibility so that the photochromic reaction can efficiently take place.

Regarding potential applications, in terms of writing and reading stored information on photochromic materials, the nonresonant character of NLO enables reading outside the absorption band. Thus, erasure during reading can be avoided. Another possible application deals with the quasi-phase-matching structure, which can be obtained by switching. To the best of our knowledge, quasi-phase-matching based on alternation of two molecular species, one obtained by isomerization of the other, has never been realized.

VII. Conclusion and Outlook

Besides the change of their UV−vis absorption spectra, photochromic molecules offer a large panel of very unusual linear and nonlinear optical properties. Scheme 1 summarizes the photoinduced effects of photochromic materials which have been described. The excitation of polymers containing azoaryls or spiropyrans with polarized light leads to transient or permanent dichroism and birefringence. For non centrosymmetric photochromes, the combination of polarized light and a static electric field leads to poled materials having second-order NLO properties. The irradiation with two coherent beams at ω and 2ω leads to all-optical poling. Irradiation of azo materials with an interference pattern yields stable surface relief gratings. Irradiation of photochromes initially poled in a solid matrix allows photoswitching of the second- or third-order NLO response, and/or annihilation of this response, depending on the matrix.

Among all existing photochromic materials, azo polymers and azo-containing hybrid materials have been particularly studied for their optical properties: the photoinduced phenomena are in general efficient, due to the trans → cis isomerization reaction, which proceeds reversibly with high quantum yields even in solid matrixes. In particular, it is remarkable that the reversibility of the trans−cis isomerization reaction of some azo compounds does not lead to a vanishing of the different photoinduced effects, such as photoinduced anisotropy and optical poling. There have been a limited number of studies dealing with other photochromic compounds; however, spiropyrans, diarylethenes, fulgides, and anils are also worthwhile to consider for some of these linear and nonlinear optical properties. The photochemical stability of fulgides and diarylethenes is particularly interesting for applications where cyclability of the photochrome is needed. Conversely, photobleaching of azo compounds by UV exposure of

Scheme 1. Photoinduced Changes of Photochromic Molecules in Polymers

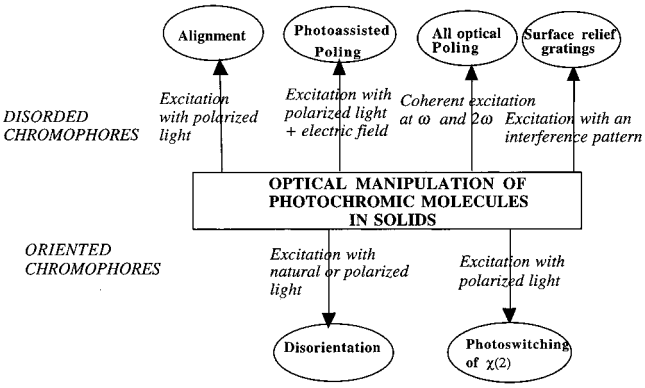

polymer or sol–gel films may be used for channel waveguide fabrication.[126,241]

Photoinduced anisotropy in liquid crystalline and amorphous polymers can be applied for reversible optical data storage: the photoinduced birefringence can be read out of the absorption wavelength of the photochrome, which prevents the erasure of the written information. Cooperative effects existing in liquid crystalline polymers lead to more efficient optical recording media. Photoinduced birefringence can also lead to holographic recording; in addition, the possibility to inscribe surface relief gratings in azo polymers after irradiation by nanosecond pulses of low fluence opens the door to applications such as real time holography.[147] A great deal of synthetic work has been done to incorporate photochromes in polymers, as either main-chain or side-chain groups, with spacers of different lengths in the last case, and the studies of the influence of molecular interactions of photochromes with the matrix environment and of relaxation processes in all the orientation phenomena described above is an emerging field.[242,243] The knowledge of these interactions is necessary if one wants to optimize both photoinduced ordering effects and stability of the optically inscribed information. The incorporation of photochromes in sol–gels or their organization in self-assembled monolayers also offers other optical materials with new optical properties.

The combination of photochromism and NLO properties in molecules leads to new macroscopic effects, such as PAP, AOP, and photoswitching of $\chi^{(2)}$. As for thermally assisted poling of NLO materials, PAP still requires an electrostatic field, but can be performed at room temperature, which is interesting for the fabrication of NLO active optical waveguides, or quasi-phase-matched structures adapted for SHG. All-optical poling is also an emerging method of poling which can be applied to octupolar molecules. Octupolar structures present some favorable features compared with dipolar ones: first, their more globular shape, without any dielectric dipole, should ease their packing in a single crystalline lattice in noncentrosymmetric arrangement; second, oriented structures (such as trigonal lamellar) of octupoles allow efficient electrooptical modulation in TE as well as TM modes, which is very convenient for devices in optical telecommunications.[165] The synthesis of octupolar molecules bearing photochromic groups will be an exciting field of research in the very near future. Finally, optical switching of $\chi^{(2)}$ is a new method which opens the door to all-optical modulation: for this purpose, the search for efficient second-order NLO active and photochromic crystals seems a promising route. The complete reversibility of the orientation of photochromes after changing from one form to the other one in amorphous matrixes seems to be more difficult to achieve, or implies short-range interactions with the matrix (hydrogen bonding, electrostatic interactions). Finally, the incorporation of photochromic molecules in photorefractive polymers[244] could lead to new materials combining several properties (second-order NLO, photoconductivity, and photochromism), which has the potential to achieve reversible and efficient refractive index modulations.

VIII. References

(1) Dürr, H.; Bouas-Laurent, H. *Photochromism: Molecules and Systems*; Elsevier: Amsterdam, 1992.
(2) Brown, G. H. Photochromism. *Techniques of Chemistry*; Wiley-Interscience: New York, 1971; Vol. III.
(3) Shinkai, S.; Manabe, O. *Top. Curr. Chem.* **1984**, *121*, 67.
(4) Kawai, S. H., Gilat, S. L.; Lehn, J.-M. *J. Chem. Soc., Chem. Commun.* **1994**, 1011.
(5) Saika, T.; Irie, M.; Shimidzu, T. *J. Chem. Soc., Chem. Commun.* **1994**, 2123.
(6) Irie, M. *Adv. Polym. Sci.* **1990**, *94*, 27.
(7) Irie, M. In *Applied Photochromic Polymer Systems*; McArdle, C. B., Ed.; Blackie: Glasgow, 1992; p 174.
(8) McArdle, C. B. In *Applied Photochromic Polymer Systems*; McArdle, C. B., Ed.; Blackie: Glasgow, 1992; p 1.
(9) Xie, S.; Natansohn, A.; Rochon, P. *Chem. Mater.* **1993**, *5*, 403.
(10) Rochon, P.; Batalla, E.; Natansohn, A. *Appl. Phys. Lett.* **1995**, *66*, 136.
(11) Kim, D. Y.; Li, L.; Kumar, J.; Tripathy, S. K. *Appl. Phys. Lett.* **1995**, *66*, 1166.
(12) Burland, D. M. *Chem. Rev.* **1994**, *94*, 1.
(13) Nalwa, H. S.; Miyata, S. In *Nonlinear Optics of Organic Molecules and Polymers*; Nalwa, H. S., Miyata, S., Eds.; CRC Press: Boca Raton, FL, 1997; Preface.
(14) Atassi, Y.; Chauvin, J.; Delaire, J. A.; Delouis, J.-F.; Fanton-Maltey, I.; Nakatani, K. *Mol. Cryst. Liq. Cryst. Sci. Technol., A* **1998**, *315*, 313.
(15) Atassi, Y.; Chauvin, J.; Delaire, J. A.; Delouis, J.-F.; Fanton-Maltey, I.; Nakatani, K. *Pure Appl. Chem.* **1998**, *70*, 2157.
(16) Weigert, F. *Verh. Phys. Ges.* **1919**, *21*, 485.
(17) Weigert, F. *Z. Phys.* **1921**, *5*, 410.
(18) Neporent, N. S.; Stolbova, O. V. *Opt. Spectrosc.* **1961**, *10*, 146.
(19) Neporent, N. S.; Stolbova, O. V. *Opt. Spectrosc.* **1963**, *14*, 331.
(20) Todorov, T.; Nikolova, L.; Tomova, N. *Appl. Opt.* **1984**, *23*, 4309.
(21) Todorov, T.; Nikolova, L.; Tomova, N. *Appl. Opt.* **1984**, *23*, 4588.
(22) Sekkat, Z.; Knoll, W. *Adv. Photochem.* **1997**, *22*, 117.
(23) Hosotte, S.; Dumont, M. *SPIE Proc.* **1996**, *2852*, 53.
(24) El Osman, A.; Dumont, M. *Polym. Prepr.* **1998**, *39*, 1036.
(25) Dumont, M.; El Osman, A. *Chem. Phys.* **1999**, *245*, 437.
(26) Dumont, M. *Mol. Cryst. Liq. Cryst.* **1996**, *282*, 437.
(27) Lagugné Labarthet, F. and Sourisseau, C. *New J. Chem.* **1997**, *21*, 879–887.
(28) El Osman, A.; Dumont, M. *SPIE Proc.* **1998**, *3417*, 36.
(29) Rochon, P.; Gosselin, J.; Natansohn, A.; Xie, S. *Appl. Phys. Lett.* **1992**, *60*, 4.
(30) Song, O. K.; Wang, C. H.; Pauley, M. A. *Macromolecules* **1997**, *30*, 6913.
(31) Biteau, J.; Chaput, F.; Lahlil, K.; Boilot, J.-P.; Tsivgoulis, G. M.; Lehn, J.-M.; Darracq, B.; Marois, C.; Lévy, Y. *Chem. Mater.* **1998**, *10*, 1945.
(32) Eich, M.; Wendorff, J. H.; Reck, B.; Ringsdorf, H. *Makromol. Chem., Rapid Commun.* **1987**, *8*, 59.
(33) Eich, M.; Wendorff, J. *J. Opt. Soc. Am. B* **1990**, *7*, 1428.
(34) Dumont, M.; Morichère, D.; Sekkat, Z.; Levy, Y. *SPIE Proc.* **1991**, *1559*, 127.
(35) Sekkat, Z.; Knoll, W. *SPIE Proc.* **1997,** *2998*, 164.
(36) Paik, C.; Morawetz, H. *Macromolecules* **1972**, *5*, 171.
(37) Smets, G. *Pure Appl. Chem.* **1975**, *42*, 509.
(38) Rau, H. In *Photochemistry and Photophysics*, Rabek, J. F., Ed.; CRC Press: Boca Raton, 1990; Vol. II, Chapter 4, p 119.
(39) Ichimura, K.; Hayashi, Y.; Akiyama, H.; Ikeda, T.; Ishizuki, N. *Appl. Phys. Lett.* **1993**, *63*, 449.
(40) Loucif-Saïbi, R.; Nakatani, K.; Delaire, J. A.; Dumont, M.; Sekkat, Z. *Chem. Mater.* **1993**, *5*, 229.
(41) Pedersen, T. G.; Ramanujam, P. S.; Johansen, P. M.; Hvilsted, S. *J. Opt. Soc. Am. B* **1998**, *15*, 272.
(42) Eich, M.; Wendorff, J. H. *Makromol. Chem., Rapid Commun.* **1987**, *8*, 467.
(43) Eich, M.; Wendorff, J. H. *J. Opt. Soc. Am. B* **1990**, *7*, 1428.
(44) Stumpe, J.; Muller, L.; Kreysig, D.; Hauck, G.; Koswig, H. D.; Ruhmann, R. D.; Rubner, J. *Makromol. Chem., Rapid Commun.* **1991**, *12*, 81.
(45) Wiesner, U.; Reynolds, N.; Boeffel, C.; Spiess, H. W. *Makromol. Chem., Rapid Commun.* **1992**, *92*, 403.
(46) Ivanov, S.; Yakovlev, I.; Kostromin, S.; Shibaev, V.; Läsker, L.; Stumpe, J.; Kreysig, D. *Makromol. Chem., Rapid Commun* **1991**, *12*, 709.
(47) Nikolova, L.; Todorov, T.; Ivanov, M.; Andruzzi, F.; Hvilsted, S.; Ramanujam, P. S. *Appl. Opt.* **1996**, *35*, 3835.
(48) Holme, N. C. R.; Ramanujam, P. S.; Hvilsted, S. *Appl. Opt.* **1996**, *35*, 5, 4622.
(49) Holme, N. C. R.; Ramanujam, P. S.; Hvilsted, S. *Opt. Lett.* **1996,** *21*, 902.

(50) Holme, N. C. R.; Nikolova, L.; Ramanujam, P. S.; Hvilsted, S. *Appl. Phys. Lett.* **1997**, *70*, 1518.
(51) Petri, A.; Kummer, S.; Anneser, H.; Feiner, F.; Bräuchle, C. *Ber. Bunsen-Ges. Phys. Chem.* **1993**, *97*, 1281.
(52) Anderle, K.; Birenheide, R.; Werner, M. J. A.; Wendorff, J. H. *Liq. Cryst.* **1991**, *9*, 691.
(53) Jones, C. and Day, S. *Nature* **1991**, *351*, 15.
(54) Bertelson, R. C.; Läsker, L.; Czapla, S.; Rübner, J.; Stumpe, J. *Mol. Cryst. Liq. Cryst. Sci. Technol., A* **1997**, *297*, 489.
(55) Fischer, T.; Läsker, L.; Rutloh, M.; Czapla, S.; Stumpe, J. *Mol. Cryst. Liq. Cryst. Sci. Technol., A* **1997**, *299*, 293.
(56) Eckardt, T.; Rutloh, M.; Stumpe, J.; Krüger, H. *J. Inf. Rec. Mater.* **1998**, *24*, 369.
(57) Natansohn, A.; Rochon, P.; Meng, X.; Barrett, C.; Buffeteau, T.; Bonenfant, S.; Pézolet, M. *Macromolecules* **1998**, *31*, 1155.
(58) Natansohn, A.; Rochon, P.; Gosselin, J.; Xie, S. *Macromolecules* **1992**, *25*, 2268.
(59) Natansohn, A.; Xie, S.; Rochon, P. *Macromolecules* **1992**, *25*, 5531.
(60) Natansohn, A.; Rochon, P.; Pezolet, M.; Audet, P.; Brown, D.; To, S. *Macromolecules* **1994**, *27*, 2580.
(61) Brown, D.; Natansohn, A.; Rochon, P. *Macromolecules* **1995**, *28*, 6116.
(62) Natansohn, A.; Rochon, P.; Ho, M.-S.; Barrett, C. *Macromolecules* **1995**, *28*, 4179.
(63) Ho, M.-S.; Natansohn, A.; Rochon, P. *Macromolecules* **1995**, *28*, 6124.
(64) Ho, M.-S.; Natansohn, A.; Barrett, C.; Rochon, P. *Can. J. Chem.* **1995**, *73*, 1773.
(65) Ho, M.-S.; Natansohn, A.; Rochon, P. *Macromolecules* **1996**, *29*, 44.
(66) Meng, X.; Natansohn, A.; Barrett, C.; Rochon, P. *Macromolecules* **1996**, *29*, 946.
(67) Meng, X.; Natansohn, A.; Rochon, P. *J. Polym. Sci., B* **1996**, *34*, 1461.
(68) Meng, X.; Natansohn, A.; Rochon, P. *Polymer* **1997**, *38*, 2677.
(69) Sekkat, Z.; Morichere, D.; Dumont, M.; Loucif-Saïbi, R.; Delaire, J. A. *J. Appl. Phys.* **1992**, *71*, 1543.
(70) Dumont, M.; Sekkat, Z. *SPIE Proc.* **1992**, *1774*, 188.
(71) Dumont, M.; Sekkat, Z.; Loucif-Saibi, R.; Nakatani, K.; Delaire, J. A. *Mol. Cryst. Liq. Cryst. Sci. Technol., B* **1993**, *5*, 395.
(72) Sekkat, Z.; Dumont, M. *Synth. Met.* **1993**, *54*, 373.
(73) Dumont, M.; Hosotte, S.; Froc, G.; Sekkat, Z. *SPIE Proc.* **1993**, *2042*, 2.
(74) Dumont, M.; Froc, G.; Hosotte, S. *Nonlinear Opt.* **1995**, *9*, 327.
(75) Dumont, M. In *The Polymeric Materials Encyclopedia*; Salamon, J. C., Ed.; CRC Press: Boca Raton, FL, 1996; p 245.
(76) Blanche, P.-A.; Lemaire, Ph.-C.; Maertens, C.; Dubois, P.; Jérôme, R. *Opt. Commun.* **1997**, *139*, 92.
(77) Sekkat, Z.; Büchel, M.; Orendi, H.; Menzel, H.; Knoll, W. *Chem. Phys. Lett.* **1994**, *220*, 497.
(78) Sekkat, Z.; Wood, J.; Knoll, W. *J. Phys. Chem.* **1995**, *99*, 17226.
(79) Sekkat, Z.; Wood, J.; Aust, E. F.; Knoll, W.; Volksen, W.; Miller, R. D. *J. Opt. Soc. Am. B* **1996**, *13*, 1713.
(80) Sekkat, Z.; Wood, J.; Knoll, W.; Volksen, W.; Miller, R. D.; Knœsen, A. *J. Opt. Soc. Am. B* **1997**, *14*, 829.
(81) Sekkat, Z.; Prêtre, P.; Knœsen, A.; Volksen, W.; Lee, V. Y.; Miller, R. D.; Wood, J.; Knoll, W. *J. Opt. Soc. Am. B* **1998**, *15*, 401.
(82) Natansohn, A.; Rochon, P.; Barrett, C.; Hay, A. *Chem. Mater.* **1995**, *7*, 1612.
(83) Hore, D.; Natansohn, A.; Rochon, P. *Can. J. Chem.* **1998**, *76*, 1648.
(84) Natansohn, A.; Rochon, P. *Macromolecules* **1998**, *31*, 7960.
(85) Rochon, P.; Bissonnette, D.; Natansohn, A.; Xie, S. *Appl. Opt.* **1993**, *32*, 7277.
(86) Ishitobi, H.; Sekkat, Z.; Kawata, S. *Chem. Phys. Lett.* **1999**, *300*, 421.
(87) Blair, H. S.; McArdle, C. B. *Polymer* **1984**, *25*, 100; **1984**, *25*, 1347.
(88) Ichimura, K.; Suzuki, Y.; Seki, T.; Hosoki, A.; Aoki, K. *Langmuir* **1988**, *4*, 1214.
(89) Sagiv, J. *J. Am. Chem. Soc.* **1980**, *102*, 92.
(90) Sekkat, Z.; Woods, J.; Geerts, Y.; Knoll, W. *Langmuir* **1996**, *12*, 2976.
(91) Sekkat, Z.; Woods, J.; Geerts, Y.; Knoll, W. *Langmuir* **1995**, *11*, 2856.
(92) Yokoyama, S.; Kakimoto, M.; Imai, Y. *Mol. Cryst. Liq. Cryst.* **1993**, *227*, 295.
(93) Ledoux, I.; Josse, D.; Zyss, J.; McLean, T.; Hann, R. A.; Gordon, P. F.; Allen, S.; Lupo, D.; Prass, W.; Scheunemann, U.; Laschewsky, A.; Ringsdorf, H. in *Nonlinear Optical Effects in Organic Polymers*; Messier, J., Kajzar, F., Prasad, P., Ulrich, D., Eds.; NATO ASI Series; Kluwer Academic Publishers: Dordrecht, The Netherlands, 1989; Vol. 162, p 79.
(94) Swalen, J. D. *J. Mol. Electron.* **1986**, *2*, 155.
(95) Knoll, W. *Makromol. Chem.* **1991**, *192*, 2827.
(96) Sekkat, Z.; Knoll, W. in *Advances in Photochemistry*; Neckers, D. C., Volman, D. H., von Bunau, G., Eds.; J. Wiley & Sons: New York, 1997; Vol. 22, p 17.
(97) Menzel, H.; Weichart, B. *Thin Solid Films* **1994**, *242*, 56.
(98) Menzel, H.; Weichart, B.; Büchel, M.; Knoll, W. *Mol. Cryst. Liq. Cryst.* **1994**, *246*, 397.
(99) Büchel, M.; Sekkat, Z.; Paul, S.; Weichart, B.; Menzel, H.; Knoll, W. *Langmuir* **1995**, *11*, 2856.
(100) Sekkat, Z.; Wood, J.; Geerts, Y.; El Meskini, A.; Büchel, M.; Knoll, W. *Synth. Met.* **1996**, *81*, 281.
(101) Hosotte, S.; Dumont, M. *Synth. Met.* **1996**, *81*, 125−127.
(102) Sekkat, Z.; Knoll, W. *Ber. Bunsen-Ges. Phys. Chem.* **1994**, *98*, 1231.
(103) Dumont, M. In *Photoactive Organic Materials, Science and Applications*; Kajzar, F., Ed.; NATO ASI Series; Kajzar, F., Ed.; Kluwer Academic Publishers: Dordrecht, The Netherlands, 1996; Vol. 9, p 501.
(104) Dumont, M. *Nonlinear Opt.* **1996**, *15*, 69.
(105) Hvilsted, S.; Andruzzi, F.; Ramanujam, P. S. *Opt. Lett.* **1992**,*17*, 1234.
(106) Ramanujam, P. S.; Hvilsted, S.; Andruzzi, F. *Appl. Phys. Lett.* **1993**, *62*, 1041.
(107) Fei, H.; Wei, Z.; Wu, P.; Han, L.; Zhao, Y.; Che, Y. *Opt. Lett.* **1994**, *19*, 411; **1994**, *19*, 1792.
(108) Lee, J. G.; Kim, D.; Lee, M. *Appl. Opt.* **1995**, *34*, 138.
(109) Bach, H.; Anderle, K.; Fuhrmann, Th.; Wendorff, J. H. *J. Phys. Chem.* **1996**, *100*, 4135.
(110) Wiesner, U.; Reynolds, N.; Boeffel, C.; Spiess, H. W. *Makromol. Chem., Rapid Commun.* **1991**, *12*, 457.
(111) Lagugné Labarthet, F.; Sourisseau, C. *J. Raman Spectrosc.* **1996**, 27, 491.
(112) Lasker, L.; Fischer, Th.; Stumpe, J.; Ruhmann, R. *J. Inf. Rec. Mater.* **1994**, *21*, 635.
(113) Buffeteau, T.; Pézolet, M. *Mikrochim. Acta* [*Suppl.*] **1997**,*14*, 395
(114) Buffeteau, T.; Pézolet, M. *Macromolecules* **1998**, *31*, 2631.
(115) Buffeteau, T.; Lagugné Labarthet, F.; Pézolet, M.; Sourisseau, C. *Macromolecules* **1998**, *31*, 7312.
(116) Pézolet, M.; Pellerin, C.; Prud′homme, R. E.; Buffeteau, T. *Vib. Spectrosc.* **1998**, *18*, 103.
(117) Tawa, K.; Kamada, K.; Sakaguchi, T.; Ohta, K. *Appl. Spectrosc.* **1998**, *52*, 1536.
(118) Bieringer, T.; Wuttke, R.; Haarer, D.; Geβner, U.; Rübner, J. *Macromol. Chem. Phys.* **1995**, *196*, 1375.
(119) Han, Y.-K.; Kim, D. Y.; Kim, Y. H. *Mol. Cryst. Liq. Cryst.* **1994**, *254*, 445.
(120) Zilker, S. J.; Bieringer, T.; Haarer, D.; Stein, R. S.; Van Egmond, J. W.; Kostromine, S. G. *Adv. Mater. (Weinheim, Ger.)* **1998**, *10*, 855.
(121) Eichmans, J.; Bieringer, T.; Kostromine, S.; Berneth, H.; Thoma, R. *Jpn. J. Appl. Phys.* **1999**, *38*, 1835.
(122) Zilker, S. J., Huber, M. R.; Bieringer, T.; Haarer, D. *Appl. Phys. B* **1999**, *68*, 893.
(123) Shi, Y.; Steier, W. H.; Yu, L.; Chen, M.; Dalton, L. *Appl. Phys. Lett.* **1991**, *59*, 2935.
(124) Teng, C. C.; Mortazavi, M. A.; Boughounian, G. K. *Appl. Phys. Lett.* **1995**, *66*, 667.
(125) Diemeer, M. B.; Suyten, F. M. M.; Trommel, E. S.; McDonach, A.; Copeland, J. M.; Jenneskens, L. W.; Horsthuis, W. H. G. *Electron. Lett.* **1990**, *26*, 379.
(126) Beeson, K. W.; Horn, K. A.; McFarland; Yardley, J. T. *Appl. Phys. Lett.* **1991**, *58*, 1955.
(127) Lee, S.-S.; Garner, S.; Steier, W. H.; Shin, S.-Y. *Appl. Opt.* **1999**, *38*, 530.
(128) Ivanov, M.; Todorov, T.; Nikolova, L.; Tomova, N.; Dragostinova, V. *Appl. Phys. Lett.* **1995**, *66*, 2174.
(129) Tanio, N.; Irie, M. *Jpn. J. Appl. Phys.* **1994**, *33*, 1550; **1994**, *33*, 3942; *J. Photochem. Photobiol., A* **1996**, *95*, 265.
(130) Boilot, J.-P.; Biteau, J.; Chaput, F.; Gacoin, T.; Brun, A.; Darracq, B.; Georges, P.; Lévy, Y. *Pure Appl. Opt.* **1998**, *7*, 169.
(131) Rochon, P.; Mao, J.; Natansohn, A.; Batalla, E. *Polym. Prepr.* **1994**, *35*, 154.
(132) Rochon, P.; Batalla, E.; Natansohn, A. *Appl. Phys. Lett.* **1995**, *66*, 136.
(133) Kim, D. Y.; Tripathy, S. K.; Li, L.; Kumar, J. *Appl. Phys. Lett.* **1995**, *66*, 1166.
(134) Kim, D. Y.; Li, L.; Jiang, X.; Shivshankar, V.; Kumar, J.; Tripathy, S. K. *Macromolecules* **1995**, *28*, 8835.
(135) Tripathy, S. K.; Kim, D. Y.; Jiang, X. L.; Li, L.; Lee, T.; Wang, X.; Kumar, J. *Mol. Cryst. Liq. Cryst. Sci. Technol., A* **1998**, *314*, 245.
(136) Lagugné Labarthet, F.; Buffeteau, T.; Sourisseau, C. *J. Phys. Chem. B* **1998**, *102*, 2654.
(137) Jiang, X. L.; Li, L.; Kumar, J.; Kim, D. Y.; Tripathy, S. K. *Appl. Phys. Lett.* **1998**, *72*, 2502.
(138) Barrett, C. J.; Natansohn, A. L.; Rochon, P. L. *J. Phys. Chem.* **1996**, *100*, 8836.
(139) Lefin, P.; Fiorini, C.; Nunzi, J.-M. *Pure Appl. Opt.* **1968**, *7*, 71.
(140) Lefin, P.; Fiorini, C.; Nunzi, J.-M. *Opt. Mater.* **1998**, *9*, 323.
(141) Jiang, X. L.; Li, L.; Kumar, J.; Kim, D. Y.; Shivshankar, V.; Tripathy, S. K. *Appl. Phys. Lett.* **1996**, *69*, 2618.
(142) Ramanujam, P. S.; Holme, N. C. R.; Hvilsted, S. *Appl. Phys. Lett.* **1996**, *68*, 1329.

(143) Holme, N. C. R.; Nikolova, L.; Ramanujam, P. S.; Hvilsted, S. *Appl. Phys. Lett.* **1997**, *70*, 1518.
(144) Lagugné Labarthet, F.; Buffeteau, T.; Sourisseau, C. *J. Phys. Chem. B* **1998**, *102*, 5754.
(145) Barrett, C. J.; Rochon, P. L.; Natansohn, A. *J. Chem. Phys.* **1998**, *109*, 1505.
(146) Lagugné Labarthet, F.; Rochon, P.; Natansohn, A. *Appl. Phys. Lett.* **1999**, *75*, 1377.
(147) Ramanujam, P. S.; Pedersen, M.; Hvilsted, S. *Appl. Phys. Lett.* **1999**, *74*, 3227.
(148) Darracq, B.; Chaput, F.; Lahlil, K.; Lévy, Y.; Boilot, J.-P. *Adv. Mater.* **1998,** *10*, 1133.
(149) Pedersen, T. G.; Johansen, P. M. *Phys. Rev. Lett.* **1997**, *79*, 2470.
(150) Pedersen, T. G.; Johansen, P. M.; Holme, N. C. R.; Ramanujam, P. S. *Phys. Rev. Lett.* **1998**, *80*, 89.
(151) Kumar, J.; Li, L.; Liang, X. L.; Kim, D. Y.; Lee, T. S.; Tripathy, S. K. *Appl. Phys. Lett.* **1998**, *72*, 2096.
(152) Viswanathan, N. K.; Balasubramanian, S.; Li, L.; Kumar, J.; Tripathy, S. K. *J. Phys. Chem. B* **1998**, *102*, 6064.
(153) Lagugné Labarthet, F.; Buffeteau, T.; Sourisseau, C. *J. Phys. Chem. B* **1999**, *103*, 6690.
(154) Paterson, J.; Natansohn, A.; Rochon, P.; Calender, C. L.; Robitaille, L. *Appl. Phys. Lett.* **1996**, *69*, 3318.
(155) Xiang, X. L.; Li, L.; Kim, D. Y.; Shivshankar, V.; Kumar, J.; Tripathy, S. K. *SPIE Proc.* **1997**, *2998*, 195.
(156) Rochon, P.; Natansohn, A.; Callender, C. L.; Robitaille, L. *Appl. Phys. Lett.* **1997**, *71*, 1008.
(157) Shen, Y. R. *The Principles of Nonlinear Optics*; Wiley: New York, 1984.
(158) Zyss, J.; Chemla, D. S. in *Nonlinear Optical Properties of Organic Molecules and Crystals*; Zyss, J., Chemla, D. S., Eds.; Academic Press: Orlando, FL 1987; Vol. 1, Chapter II-1, p 23.
(159) Williams, D. J. *Nonlinear Optical Properties of Organic and Polymeric Materials*, ACS Symposium Series 233; American Chemical Society: Washington, DC, 1985.
(160) Burland, D. M.; Miller, R. D.; Walsh, C. A. *Chem. Rev.* **1994**, *94*, 31.
(161) Kanis, D. R.; Ratner, M. A.; Marks, T. J. *Chem. Rev.* **1994**, *94*, 195.
(162) Nalwa, H. S.; Watanabe, T.; Miyata, S. In *Nonlinear Optics of Organic Molecules and Polymers*; Nalwa, H. S., Miyata, S., Eds.; CRC Press: Boca Raton, FL, 1997; p 89.
(163) Levine, B. F.; Bethea, C. G. *J. Chem. Phys.* **1974**, *60*, 3856.
(164) Clays, K.; Persoons, A. *Phys. Rev. Lett.* **1991**, *66*, 2980; *Rev. Sci. Instrum.* **1992**, *63*, 3285.
(165) Zyss, J.; Ledoux, I. *Chem. Rev.* **1994**, *94*, 77.
(166) Pugh, D.; Morley, J. O. In *Nonlinear Optical Properties of Organic Molecules and Crystals*; Zyss, J., Chemla, D. S., Eds.; Academic Press: Orlando, FL, 1987; Vol. 1, Chapter II-2, p 193.
(167) Kurtz, H. A.; Stewart, J. J. P.; Dieter, K. M. *J. Comput. Chem.* **1990**, *11*, 82.
(168) Armstrong, J. A.; Bloembergen, N.; Ducuing, J.; Pershan, P. S. *Phys. Rev.* **1962**, *127*, 1918.
(169) Ward, J. F. *Rev. Mod. Phys.* **1965**, *37*, 1.
(170) Orr, B. J.; Ward, J. F. *Mol. Phys.* **1971**, *20*, 513.
(171) Morell, J. A.; Albrecht, A. C. *Chem. Phys. Lett.* **1979**, *64*, 46.
(172) Pugh, D.; Morley, J. O. *Nonlinear Opt. Prop. Org. Mol. Cryst.* **1987**, *1*, 193.
(173) Katz, H. E.; Dirk, C. W.; Singer, K. D., Sohn, J. E. *SPIE Proc.* **1987**, *824*, 86.
(174) Katz, H. E.; Singer, K. D., Sohn, J. E.; Dirk, C. W.; King, L. A.; Gordon, H. M. *J. Am. Chem. Soc.* **1987**, *109*, 6561.
(175) Albert, I. D. L.; Morley, J. O.; Pugh, D. *J. Phys. Chem.* **1995**, *99*, 8024.
(176) Kongrauz, V. In *Applied Photochromic Polymer Systems*; McArdle, C. B., Ed.; Blackie: Glasgow, 1992; p 21.
(177) Atassi, Y.; Delaire, J. A.; Nakatani, K. *J. Phys. Chem.* **1995**, *99*, 16320.
(178) Nakatani, K.; Atassi, Y.; Delaire, J. A. *Nonlinear Opt.* **1996**, *15*, 351.
(179) Chauvin, J.; Delaire, J. A.; Fanton-Maltey, I.; Irie, M.; Nakatani, K. *Mol. Cryst. Liq. Cryst.*, in press.
(180) Gilat, S. L.; Kawai, S. H.; Lehn, J.-M. *Chem. Eur. J.* **1995**, *1*, 275.
(181) Nakatani, K.; Delaire, J. A. *Chem. Mater.* **1997**, *9*, 2682.
(182) Houbrechts, S.; Clays, K.; Persoons, A.; Prikamenou, Z.; Lehn, J.-M. *Chem. Phys. Lett.* **1996**, *258*, 485.
(183) Meredith, G. R.; Krongauz, V.; Williams, D. J. *Chem. Phys. Lett.* **1982**, *87*, 289.
(184) Yitzchaik, S.; Berkovic, G.; Krongauz, V. *Chem. Mater.* **1990**, *2*, 162.
(185) Yitzchaik, S.; Berkovic, G.; Krongauz, V. *Macromolecules* **1990**, *23*, 3539.
(186) Yitzchaik, S.; Berkovic, G.; Krongauz, V. *Adv. Mater.* **1990**, *2*, 33.
(187) Eich, M.; Looser, H.; Yoon, D.; Twieg, R.; Bjorklund, G.; Baumert, J. *J. Opt. Soc. Am. B* **1989**, *6*, 1590.
(188) Sekkat, Z.; Dumont, M. *Appl. Phys. B* **1992**, 54, 486.
(189) Sekkat, Z.; Dumont, M. *Mol. Cryst. Liq. Cryst. B* **1992**, *2*, 359.
(190) Sekkat, Z.; Knoll, W. *J. Opt. Soc. Am. B* **1995**, *12*, 1855.
(191) Delaire, J. A.; Atassi, Y.; Loucif-Saïbi, R.; Nakatani, K. *Nonlinear Opt.* **1995**, *9*, 317.
(192) Palto, S. P.; Blinov, L. M.; Yudin, S. G.; Grewer, G.; Schönhoff, M.; Lösche, M. *Chem. Phys. Lett.* **1993**, *202*, 308.
(193) Blinov, L. M.; Barnik, M. I.; Weyrauch, T.; Palto, S. P.; Tevesov, A. A.; Haase, W. *Chem. Phys. Lett.* **1994**, *231*, 246.
(194) In the symmetry of poled materials poled along an axis (z), there are only two different quadratic nonlinear coefficients, namely, $\chi^{(2)}_{zzz}$ and $\chi^{(2)}_{zxx}$. In the case of SHG, half values of these coefficients are also noted, respectively d_{33} and d_{31}.
(195) Loucif-Saïbi, R.; Dhénaut, C.; Nakatani, K.; Delaire, J. A. *Mol. Cryst. Liq. Cryst.* **1993**, *235*, 251.
(196) El Osman, A.; Dumont, M. *Macromol. Symp.* **1999**, *137*, 137.
(197) Hill, R. A.; Dreher, S.; Knoesen, A.; Yankelevitch, D. R. *Appl. Phys. Lett.* **1995**, *66*, 2156.
(198) Atassi, Y.; Loucif-Saïbi, R.; Nakatani, K.; Delaire, J. A. *Mol. Cryst. Liq. Cryst.* **1994**, *246*, 355.
(199) Sekkat, Z.; Kang, C. S.; Aust, E. F.; Wegner, G.; Knoll, W. *Chem. Mater.* **1995**, *7*, 142.
(200) Nakatani, K.; Atassi, Y.; Delaire, J. A.; Guglielmetti, R. *Nonlinear Opt.* **1994**, *8*, 33.
(201) Williams, M. L.; Landel, R. F.; Ferry, J. D. J. *Am. Chem. Soc.* **1955**, *77*, 3701.
(202) Williams, G.; Watts, D. C. *Trans. Faraday Soc.* **1970**, *66*, 80.
(203) Chen, T.-A.; Jen, A.-Y.; Cai, Y. *Macromolecules* **1996**, *29*, 535.
(204) Yu, D.; Gharavi, A.; Yu, L. *Macromolecules* **1996**, *29*, 6139.
(205) Harris, F. W.; Li, F.; Lin, S.-H.; Chen, J.-C., Cheng, S. Z. D. *Macromol. Symp.* **1997**, *122*, 33.
(206) Lee, H.-J.; Lee, M.-H.; Han, S.-G.; Kim, H.-Y., Ahn, J.-H.; Lee, E.-M.; Won, Y.-H. *J. Polym. Sci., A* **1998**, *26*, 301.
(207) Miller, R. D.; Burland, D. M.; Jurich, M. C.; Lee, V. Y.; Moylan, C. R.; Thackara, J.; Twieg, R. J.; Verbiest, T.; Volksen, W. *Macromolecules* **1995**, *28*, 4970.
(208) Chauvin, J.; Nakatani, K.; Delaire, J. A. *SPIE Proc.* **1997**, *2998*, 205.
(209) Sekkat, Z.; Knoesen, A.; Lee, V. Y.; Miller, R. D.; Wood, J., Knoll, W. In *Organic Thin Films Structures and Applications*; Frank, C. W., Ed.; ACS Symposium Series; American Chemical Society: Washington, DC, 1997; p 295.
(210) Sekkat, Z.; Knoesen, A.; Lee, V. Y., Miller, R. D. *J. Polym. Sci., B* **1998**, *36*, 1669.
(211) Chauvin, J.; Delaire, J. A.; Nakatani, K. *Mol. Cryst. Liq. Cryst.*, in press.
(212) Blanchard, P. M.; Mitchell, G. R. *Appl. Phys. Lett.* **1993**, *63*, 2038.
(213) Bauer-Gogonea, S.; Bauer, S.; Wirges, W.; Gerhard-Multhaupt, R. *J. Appl. Phys.* **1994**, *76*, 2627.
(214) Anneser, H.; Feiner, F.; Petri, A.; Braüchle, C.; Leigeber, H.; Weitzel, H.-P.; Kreuzer, F.-H.; Haak, O.; Boldt, P. *Adv. Mater.* **1993**, *5*, 556.
(215) Chaput, F.; Riehl, D.; Lévy, Y.; Boilot, J.-P. *Chem. Mater.* **1993**, *5*, 589.
(216) Watanabe, T.; Nalwa, H. S., Miyata, S. In *Nonlinear Optics of Organic Molecules and Polymers*; Nalwa, H. S., Miyata, S., Eds.; CRC Press: Boca Raton, FL, 1997; p 351.
(217) Yilmaz, S.; Bauer, S.; Gerhard-Multhaupt, R. *Appl. Phys. Lett.* **1994**, *64*, 2770.
(218) Bauer-Gogonea, S.; Gerhard-Multhaupt, R. *Electrets*; Laplacian Press: Morgan Hill, 1999; Chapter 14.
(219) Charra, F.; Devaux, F.; Nunzi, J.-M.; Raimond, P. *Phys. Rev. Lett.* **1992**, *68*, 2440.
(220) Charra, F.; Kajzar, F.; Nunzi, J.-M.; Raimond, P.; Idiart, E. *Opt. Lett.* **1993**, *18*, 941.
(221) Nunzi, J.-M.; Charra, F.; Fiorini, C. *Condensed Matter News* **1993**, *2*, 6.
(222) Fiorini, C.; Charra, F.; Nunzi, J.-M. *J. Opt. Soc. Am. B* **1994**, *12*, 2347.
(223) Fiorini, C.; Charra, F.; Nunzi, J.-M.; Raimond, P. *J. Opt. Soc. Am. B* **1997**, *14*, 1984.
(224) Fiorini, C.; Charra, F.; Nunzi, J.-M.; Raimond, P. *Nonlinear Opt.* **1995**, *9*, 339.
(225) Chalupczak, W.; Fiorini, C.; Charra, F.; Nunzi, J.-M., Raimond, P. *Opt. Commun.* **1996**, *126*, 103.
(226) Nunzi, J.-M.; Fiorini, C.; Etilé, A.-C.; Kajzar, F. *Pure Appl. Opt.* **1998**, *7*, 141.
(227) Fiorini, C.; Nunzi, J.-M. *Chem. Phys. Lett.* **1998**, *286*, 415.
(228) Etilé, A.-C.; Fiorini, C.; Charra, F.; Nunzi, J.-M. *Phys. Rev. A* **1997**, *56*, 3888.
(229) Si, J.; Xu, G.; Liu, X.; Yang, Q.; Ye, P.; Li, H.; La, H.; Shen, Y. *Opt. Commun.* **1997**, *142*, 71.
(230) Si, J.; Mitsuyu, T.; Ye, P.; Shen, Y.; Hirao, K. *Appl. Phys. Lett.* **1998**, *72*, 762.
(231) Xu, G.; Yang, Q. G.; Si, J.; Liu, X.; Ye, P.; Li, Z.; Shen, Y. *Opt. Commun.* **1999**, *159*, 88.
(232) Fiorini, C.; Nunzi, J.-M.; Charra, F.; Kajzar, F.; Lequan, M.; Lequan, R.-M.; Chane-Ching, K. *Chem. Phys. Lett.* **1997**, *271*, 335.

(233) Fiorini, C.; Charra, F.; Raimond, P., Lorin, A.; Nunzi, J.-M. *Opt. Lett.* **1997**, *22*, 1846.
(234) Nunzi, J.-M.; Charra, F.; Fiorini, C.; Zyss, J. *Chem. Phys. Lett.* **1994**, *219*, 349.
(235) Fiorini, C.; Charra, F.; Nunzi, J.-M.; Samuel, I. F. W.; Zyss, J. *Opt. Lett.* **1995**, *20*, 2469.
(236) Coe, B. J. *Chem. Eur. J.* **1999**, *5*, 2464.
(237) Aoki, H.; Ishikawa, K.; Takezoe, H.; Fukuda, A. *Jpn. J. Appl. Phys. A* **1996**, *35*, 168.
(238) Large, M. C. J.; Kajzar, F.; Raimond, P. *Appl. Phys. Lett.* **1998**, *73*, 3635.
(239) Yamada, K.; Otsubo, H.; Yonemura, H.; Yamada, S.; Matsuo, T. *Chem. Lett.* **1997**, 451.
(240) Sato, O.; Baba, R.; Hashimoto, K.; Fujishima, A. *Denki Kagaku* **1994**, *62*, 530.
(241) Ikegaya, K.; Miyashita, I.; Sugihara, O.; Okamoto, N.; Egami, C. In *Poled Polymers and their Applications to SHG and EO Devices*; Miyata, S., Sasabe, H., Eds.; Advances in Nonlinear Optics; Miyata, S.; Sasabe, H., Eds.; Gordon and Breach Science Publishers: Amsterdam, 1997; Vol. 4, p 231.
(242) Kaatz, P.; Prêtre, Ph.; Meier, U.; Stalder, U.; Bosshard, Ch.; Günter, P. in *Poled Polymers and their Applications to SHG and EO Devices*; Miyata, S., Sasabe, H., Eds.; Advances in Nonlinear Optics, Vol. 4; Miyata, S.; Sasabe, H., Eds.; Gordon and Breach Science Publishers: Amsterdam, 1997; Vol. 4, p 165.
(243) Winkelhahn, H.-J.; Neher, D.; Servay, Th. K., Rengel, H.; Pfaadt, M.; Böffel, C.; Schulze, M. In *Poled Polymers and their Applications to SHG and EO Devices*; Vol. 4; Miyata, S.; Sasabe, H., Eds.; Advances in Nonlinear Optics; Gordon and Breach Science Publishers: Amsterdam, 1997; Vol. 4, p 179.
(244) Kippelen, B.; Meerholz, K.; Peyghambarian, N. In *Nonlinear Optics of Organic Molecules and Polymers*; Nalwa, H. S., Miyata, S., Eds.; CRC Press: Boca Raton, FL, 1997; p 465.

CR980078M